Title:

Cerebromicrovascular disease in elderly with diabetes

Abbreviations used in this proposal

A1C	hemoglobin A1C
ACA	anterior cerebral artery
ADL	activities of daily living
BADS	behav. asses. of dysexecutive. syndr.
BFV	blood flow velocity
BIDMC	Beth Israel Deaconess Medical Center
BMI	body mass index
BP	blood pressure
CASL	continuous arterial spin labeling
CBF	cerebral blood flow
CDT	clock drawing test
CIB	clock-in-the-box
COP	center of pressure
CRP	C-reactive protein
CSF	cerebrospinal fluid
DTI	diffusion tensor imaging
FLAIR	fluid-attenuated inversion recovery
FSE	fast spin echo
GM	gray matter
GDS	geriatric depression scale
GCRC	General Clinical Research Center
HVLT-R	Hopkins verbal learning test
ICAM-1	intracellular adhesion molecule
IL6,10	interleukins 6,10
IR-FGE	inversion recovery fast gradient echo
MCA	middle cerebral artery
MRI	magnetic resonance imaging
ROCF	Rey-Ostereith complex figure
SAFE	Syncope and Falls in the Elderly Laboratory
SKF	skin fold thickness
SVCAM-1	vascular adhesion molecule
TNF α	tumor necrosis factors alpha
TCD	transcranial Doppler ultrasound
WM	white matter
WMHs	white matter hyperintensities

A. HYPOTHESIS AND SPECIFIC AIMS

Diabetes mellitus (DM) is associated with cerebral microvascular disease, increases the risk for vascular dementia and stroke,[16] and doubles the mortality rate.[17] The precise relationship between diabetes, neuroanatomical changes, and functional outcomes remains unknown. Diabetes alters the permeability of the blood-brain barrier, thus affecting regional metabolism and microcirculatory regulation.[18] Hyperglycemia and pro-inflammatory cytokines are the leading causes of endothelial dysfunction and neuronal cell damage.[19] Specifically, it appears that the fronto-temporal cortex [20] and periventricular white matter (WM)[18] are particularly vulnerable to diabetic metabolic disturbance and hypoperfusion. Neuroanatomical changes in these structures have consequences for memory, executive functions, and balance in the elderly.[21,22] **Our goals for this study are to determine prospectively the impact of type 2 diabetes on cerebral perfusion and brain tissue damage and the consequences for cognition and balance in older adults.** We plan to investigate these relationships prospectively via quantitative measures of cerebral perfusion and vasoregulation using MRI and transcranial Doppler ultrasound and to determine their long-term clinical impact in diabetic and control subjects over 2 years of follow-up. This study will provide invaluable data about the effects of diabetes on cerebral perfusion that can translate into new diagnostic markers and therapeutic targets for management of diabetic brain damage. We propose the following Specific Aims:

Hypothesis 1: Hyperglycemia is a common mechanism for microvascular disease, disturbance in blood flow regulation, and brain tissue damage in older adults with type 2 diabetes.

Aim 1a: To determine the effects of type 2 DM on regional gray and white matter and cerebrospinal fluid (CSF) volumes, using a segmentation method applied on T1- and T2- weighted images, and on perfusion maps, measured using continuous arterial spin labeling (CASL) images at 3 Tesla MRI.

Aim 1b: To determine the effects of type 2 DM on the dynamics of cerebral vasoregulation from responses of cerebral blood flow velocities (BFV) in anterior and middle cerebral arteries (ACA and MCA) measured by Doppler ultrasound during CO_2 challenges and orthostatic stress. We aimed to study 60 patients with type 2 DM and 60 matched controls aged 50-85 years.

Hypothesis 2: Inflammation contributes to neuroanatomical changes in periventricular white matter and white matter hyperintensities on MRI.

Aim 2: To determine the association between inflammation markers and white matter integrity, we measured WM atrophy, anisotrophy, and hyperintensities (WMHs) using fluid attenuated inversion recovery (FLAIR) and diffusion tensor (DTI) imaging at 3 Tesla MRI in the diabetic and control groups.

Hypothesis 3: Cortical and subcortical atrophy in frontal and temporal regions manifest as executive dysfunction and impairment of balance in older adults with type 2 DM. Diabetes severity increases progression of microvascular disease and brain tissue damage. Higher hemoglobin A1C is associated with accelerated decline in cerebral blood flow, cortical and subcortical brain volumes, and cognition and balance in older adults with type 2 DM.

In Aim 3 we prospectively determined the relation between diabetes, cerebral hypoperfusion and brain tissue damage, and functional outcomes over the 2-year follow-up.

Aim 3a: To determine the relationship between brain tissue volumes in the frontal and temporal regions and memory, executive function, and balance scores (the center of pressure displacement upon standing using force platform) in the diabetes and control groups.

Aim 3b: To determine longitudinally if higher hemoglobin A1C levels are associated with progression of cerebral blood flow (CBF) dysregulation, brain atrophy, and accelerated decline in functional outcome measures (cognitive and balance scores). We compared our measurements of regional perfusion and brain tissue volumes using CASL and T1- and T2-weighted MRI at 3 Tesla (as described in Aim 1) and compared cognitive and balance scores at baseline and after 2 years of follow-up in the diabetic and control groups. We used multiple regression models to determine the association between A1C and changes of regional brain volumes, regional perfusion, and cognitive and balance scores in the diabetes and control groups.

In contrast to that of a younger population, the pathophysiology of DM in elderly people has been poorly investigated and is not well understood. The fastest-growing population of older diabetic patients remains

understudied. This study will prospectively evaluate relationships among type 2 DM, cerebral perfusion, and neuroanatomical and clinical outcomes. Cerebral hypoperfusion and brain atrophy in the fronto-temporal lobes may affect executive functions, planning, and problem solving in elderly people and may ultimately feed into a vicious cycle of poor diabetes management and increased severity of the disease and its complications. Diabetes exerts long-term and continuous effects on the brain, and therefore there is an urgent clinical need to develop new biomarkers of cerebromicrovascular disease in type 2 DM and to implement them into practice guidelines and diabetes management. By determining the factors that contribute to cognitive and functional decline in older people and providing novel biomakers that can be used for early detection of impairment of cerebrovascular regulation, this proposal may have broad socioeconomic impact on aging population.

B. BACKGROUND AND SIGNIFICANCE

B.1. Diabetes: a major public health problem

There are 20.8 million people in the United States of all ages affected with DM, and 20.9% are >60 years old. The direct cost of this diabetes epidemic is $92 billion with an additional cost of $40 billion for disability, work loss, and premature mortality. In contrast to a younger population, in elderly people the pathophysiology of DM has been poorly investigated and is not well understood, and thus this fastest-growing population of older diabetic patients remains understudied.

B.2. Regional blood flow distribution and brain atrophy in diabetes

Previous studies have shown cross-sectionally that regional perfusion in the frontal and temporal lobes and other areas with higher metabolic rates are specifically affected by diabetes.[23] Cerebral blood flow (CBF) abnormalities were most frequently seen in the fronto-temporal region, followed by the occipital and parietal regions,[24] and were more frequent with long-term diabetes. Hypoperfusion was also related to fluctuating blood glucose and A1C levels and to the frequency of hypoglycemia.[25,26] In diabetic persons, the ratio between regions with normal CBF vs. reduced CBF was lower than in the controls and inversely correlated with systolic BP, total cholesterol, and atherogenic index. These observations suggest that the combination of hyperglycemia with other risk factors for atherosclerosis may accelerate age-related decline in perfusion.[27,20] During hypoglycemia CBF increased to areas associated with increased metabolic rate, cognitive and motor processing i.e. superior frontal cortices and the right thalamus and decreased to the right posterior cingulate cortex and the right putamen.[28 29] Type 2 DM is associated cross-sectionally with modest cortical and subcortical atrophy, lacunar infarcts, and asymptomatic infarcts.[30,15, 31] Cortical and subcortical atrophy was linked with diabetes duration and A1C, and with impaired attention and executive functions, processing speed, and memory. Cognitive performance was inversely related to atrophy, WMHs, and silent infarcts. There was also a modest relationship between cognitive decline, A1C, and DM duration.[1] Gray matter loss was observed in areas used for memory and language processing (superior temporal and angular gyri). Gray matter density declined with elevated lifetime A1C levels, DM duration, and diabetic retinopathy. It appears that superior temporal gyri may be particularly vulnerable to diabetes, as suggested by the relationship between A1C and atrophy in these regions.[32] Our preliminary data also showed that cortical and subcortical atrophy was more pronounced in frontal and temporal regions, and was associated with CBF reduction and impaired vasoreactivity in those regions. In diabetic patients, choline-containing compounds, indicative of neuronal loss, were increased in the WM and in the thalamus; myo-inositol was increased in the white matter, glucose excess was found throughout the brain, and water intensity was increased in the cortical voxels. Calculated lifetime glycemic exposure was correlated inversely with choline and N-acetyl-containing compounds in WM and with choline in the thalamus. An association between altered brain metabolites and glycemic control and increased concentrations of intracellular and vascular adhesion molecules suggests the presence of a vascular-mediated progressive metabolic disturbance in the brain.[18]

B.3. Cognition and postural control in diabetes

Cognitive decline, slow gait speed, and falls are common manifestations of subcortical frontal dysfunction that occurs frequently with aging. The population-based Kunsgholmen study reported that DM was associated with hazard ratios of 1.5 for dementia, 2.6 (95% CI 1.2 to 6.1) for vascular dementia, and 1.3 for Alzheimer's disease. In patients who were treated with oral antidiabetic medications, the hazard ratio increased to 1.7 (95% CI 1.0 to 2.8) for dementia and to 3.6 (CI 1.3 to 9.5) for vascular dementia. The risk for vascular dementia increased further in DM patients with severe systolic hypertension or heart disease.[16] In addition, microvascular disease and subcortical WMHs were associated cross-sectionally with cognitive impairment.[33,34,35] and longitudinally with the rate of cognitive decline[35] among community-dwelling elders. A recent longitudinal study of 224 cognitively normal subjects older than 60 years[36] showed that an increase in the WMH volume was associated with a concurrent decrease in WM perfusion, reduced frontal lobe metabolism, and lower cognitive scores.[37] Most studies suggest that patients with subcortical vascular dementia are more impaired on frontal-executive tasks than memory, i.e., free recall, as recognition or cued memory, is often well-preserved.[38] Therefore, chronic hyperglycemia may aggravate age-related vascular dysfunction, thereby leading to early degeneration of associative brain regions with higher metabolic demands involved in cognition or motor control.

Postural control and mobility. Balance in the upright position is maintained through complex mechanisms that control interactions between musculoskeletal and somatosensory systems. Displacement of the center of

pressure (COP) has been used to assess postural sway and to demonstrate the impact of aging and age-related disorders on postural control.[39,40] Increased postural sway in older adults is well-documented, and research has linked greater amounts of postural sway to an increased risk of falling, a serious problem for older adults. In diabetic persons, abnormalities in postural control and mobility are commonly attributed to impaired sensory-motor inputs due to peripheral diabetic neuropathy.[41] Increasing evidence shows that subcortical WM degeneration may contribute to psychomotor slowing and poor balance in older people even in the absence of peripheral neuropathy. In a study of more than 700 community-dwelling participants from the Cardiovascular Health Study, WMHs were associated with worse performance on tests of balance using both clinical and dynamic posturography measures.[42] Among 1077 non-demented elderly men and women participating in the Rotterdam Scan Study,[35] those with the most severe diffuse subcortical WMHs scored nearly 1 SD below the mean on tests of psychomotor speed. Whitman et al.[43] compared the progression of WMHs in people with poor postural control and in healthy subjects. Subjects whose scores dropped more than 4 points on the Tinetti Performance Oriented Mobility Score over 4 years had a greater increase in WMHs volume and number of falls than those with normal scores. In a 10-year longitudinal study, Baloh and colleagues also reported a correlation between yearly changes in the Tinetti balance score and WMHs.[44] Because of the close proximity of frontal-subcortical circuits that control both motor and cognitive functions, it is not surprising that periventricular vascular lesions may simultaneously cause dysfunction in both systems. Cerebral oxygenation in the frontal lobes declined during active standing in healthy elderly,[45] and BFV in middle cerebral arteries declined in about 30% of people with orthostatic hypotension.[46] Therefore, regional brain metabolism may be exposed to fluctuations in perfusion pressure, compromising especially the periventricular watershed areas and regions with high metabolic demands.

B.4. Contributions to current knowledge

Despite recent advances, the complex effects of diabetic metabolic disturbance on neuroanatomy and cerebral blood flow regulation are not well understood. There is growing evidence suggesting that diabetes is associated with cortical and subcortical atrophy and impaired CBF regulation.[1] Previous Doppler ultrasound and MRI studies were cross-sectional, combined both type 1 and type 2 diabetes, and were not focused on elderly people. Our studies have shown cross-sectionally that cerebral autoregulation is severely damaged in older diabetic patients.[47] Diabetics experience significant gray matter and WM atrophy and a 15% increase of cerebrospinal fluid volume as compared with healthy controls.[48] Keeping in mind that cerebral atrophy progresses at a rate of 1% per year after the age of 65, such loss of both gray and white matter indicates that diabetic brain ages faster by 15 years or more. Combined effects of neurotoxicity, endothelial dysfunction, and inflammation contribute to neurodegeneration in diabetic brain.[49, 50] A link between cognitive impairment and brain atrophy is strong, but associations between diabetes control, disease duration, and functional outcomes remain unclear.[1] Therefore, multiple pathways of neurodegeneration may work in concert: 1) endothelium-mediated defects in microvascular reactivity, blood-brain barrier disruption, and autoregulation leading to chronic hypoperfusion; 2) hyperglycemia-associated neurotoxicity, WM degeneration, and brain atrophy; and/or 3) up-regulation of inflammatory cytokines contributing to both WM demyelination and microvascular disease. Therefore, understanding these pathophysiological mechanisms is crucial for prevention and treatment of cerebrovascular complications of diabetes in older adults. Our study will address these gaps in existing knowledge and provide links between diabetes control and functional outcomes.

Innovation of proposed approach

Previous findings suggested that diabetes may lead to continuous and progressive brain tissue damage that might precede the onset of cerebrovascular complications by years. This concept, however, has not yet been validated in prospective studies. We will combine novel methodologies to provide prospective data, which are lacking, about structure-function relationships in the older diabetic population: 1) the effects of DM on structural changes in brain tissues and disruption of WM pathways using state-of-the art high resolution anatomical, perfusion, and diffusion tensor imaging techniques at 3 Tesla; 2) a link between regional differences in perfusion, vasoreactivity, and diabetes control; 3) association between inflammation, progression of WM degeneration, disruption of WM pathways, and cognitive and motor outcomes; 3) data about structure-perfusion-function relationships that will elucidate the effects of chronic hyperglycemia, diabetes control, and functional outcomes of cognition and balance; 4) statistical modeling approach will provide new insights into complex relationship

between diabetes control and other factors that may contribute to faster progression of cerebrovascular disease and functional decline in older diabetic people. This study may broadly impact scientific knowledge about the effects of diabetes on aging brain and will provide evidence-based data that can be used for development of new policies to set new targets for treatment of diabetes in the central nervous system. We expect to find that:

- Diabetes accelerates aging of the brain, and the progression of brain atrophy is even faster with uncontrolled diabetes. Brain regions with high metabolic rate, such as frontal and temporal cortices and basal ganglia, will be the first affected by diabetic metabolic disturbance and abnormalities in vasoreactivity.
- Inflammation contributes to a degeneration of WM pathways that affects preferentially frontal and temporal cortices with functional consequences for cognition and balance control. Demyelination of WM pathways, manifesting as increased fractional anisotropy on DTI images, may precede development of WM abnormalities and functional impairment. Inflammation markers may be up-regulated in patients with uncontrolled diabetes and further contribute to WM degeneration and brain atrophy.
- Dependency of cerebral BFV on peripheral BP, as indicated by reduced BP-BFV phase shift, is a novel noninvasive marker of impairment of cerebral autoregulation dynamics. Reduction of BP-BFV phase shift will precede structural MRI abnormalities and decline in functional outcomes and can be used for noninvasive monitoring of cerebromicrovascular disease progression. The combination of ultrasound and MRI technique that we propose is novel and will provide data about dynamics of CBF regulation, as well as associations among regional cerebral perfusion and regional cortical and subcortical volumes and WMH distributions in the understudied population of older diabetics.
- Factors contributing to diabetic metabolic disturbance and CBF dysregulation have additive effects.

B. 5. Clinical impact factor and relevance to broad long-term objective

The goals of the Healthy People 2010 initiative are to improve diagnostics and to prevent complications of diabetes. Type 2 DM is a complex metabolic disease arising from variable interaction of hereditary and environmental factors contributing to hyperglycemia, endothelial dysfunction, and end-organ complications. There is increasing evidence from epidemiological studies that diabetes is a risk for accelerated aging in the brain.[12] Diabetes increases the risk for stroke 2-4 times, doubles the mortality rate, and increases the risk for Alzheimer's disease and vascular dementia.[16] DM in older adults, seldom found in isolation, is usually encountered in the context of multiple metabolic disorders and vascular risk factors (hypertension, smoking, physical inactivity, dyslipidemia, and obesity). Factors predisposing to DM in elderly are age-related decrease of insulin secretion and age-related increase in insulin resistance, adiposity, co-existing illness (hyperlipidemia, hypertension, coronary artery disease, decreased physical activity, drugs, genetics, and other factors such as inflammation. Cerebral manifestations of DM in the elderly are unique, as diabetes causes further damage to neurons and cerebrovascular reserve that are already compromised by age and other risk factors, making elderly patients even more vulnerable to adverse effects of diabetic metabolic disturbance. Diabetes causes blood-brain barrier break-down and progressive brain tissue damage [12-15] that may precede cerebrovascular complications and dementia by years, but this concept has not yet been validated in prospective studies. This proposal will target pathophysiological mechanisms, including hyperglycemia and inflammatory processes, that couple endothelial dysfunction with brain tissue damage and functional outcomes in older adults with diabetes and that are unknown. Based on this evidence, prevention of diabetic brain damage needs to be incorporated in the long-term care of diabetic patients.

Impact on management of geriatric diabetes and practice guidelines

This research study will have broad implications for geriatric practice and diabetes care. Long-term goals in geriatric care for elderly are improving qualify of life, promoting independence, and prevention of dementia and strokes. Current clinical practice guidelines, however, are based on evidence-based medicine focused on a single-disease pathophysiology in middle-aged adults. [51]

- The current practice guidelines have limited applications for older individuals with multiple co-morbidities and pathophysiology, already changed by aging. Complicated polypharmacy and non-pharmacological regimes of diet and exercise are expensive and difficult to follow, thus leading to non-compliance.
- Cognitive decline and brain tissue damage need to be listed as diabetic complications.

- Cognitive assessment needs to be incorporated into treatment plans. Undiagnosed executive dysfunction affects complex tasks, such as planning and problem solving, reasoning, and attention. Psychomotor slowing and decline in motor skills contribute to falls, leading causes of disability in elderly people. Together, they impair a person's ability to understand and to manage diabetes, feeding into a vicious cycle of poor glucose control and increased severity of DM complications.
- New treatment strategies with focus on treatment of cerebral hypoperfusion, central nervous system protection, and prevention of cognitive decline need to be developed and incorporated into practice guidelines. Ideal treatments would improve cerebral autoregulation, improve insulin sensitivity, and provide neuroprotection to prevent cognitive decline and dementia.[16, 52]
- Preventive strategies need to be administered more rigorously and to target younger diabetic and older pre-diabetic populations. Older adults are more prone to hypoglycemia associated with glucose-control agents, but less aware of its symptoms. Hypoglycemia may be associated with orthostatic hypotension, cerebral hypoperfusion, and falls. Therefore, diabetes treatments need to be optimized to prevent hypoglycemia.

This proposal will provide new evidence about the effects of type 2 DM on regional brain perfusion, brain tissue volumes, and diabetes control and functional outcomes that can be used to initialize efforts to implement brain protection as a new target for prevention of diabetic complications. This proposal may have large socioeconomic impact by providing data about factors that may accelerate diabetic brain damage and functional decline that could be otherwise prevented.

C. PRELIMINARY RESULTS

In our Aims 1 and 2 we planned to determine prospectively the consequences of cerebromicrovascular disease and inflammation on perfusion and brain tissue volume that are supported by our preliminary data from cross-sectional analysis in sections C.1.-C.4.

C.1. Cerebral blood flow velocity and periventricular white matter hyperintensities in type 2 diabetes mellitus.

V. Novak, D. Last, D.C. Alsop, et al. Diabetes Care 2006;29:1529-34.

We evaluated the effects of type 2 DM on flow velocities in the MCAs and to determine the relationship between WMHs on MRI and BFV. We measured BFV in 28 type 2 DM and 22 control subjects (aged 62.3 ± 7.2 years) using TCD during baseline, hypocapnia, and hypercapnia. WMHs were graded and their volume was quantified from FLAIR images at 3 Tesla MRI. The DM group had decreased mean BFV and increased cerebrovascular resistance during baseline, hypocapnia, and hypercapnia ($p<0.0001$), and impaired CO_2 reactivity ($p=0.05$). WMH volume was negatively correlated with baseline BFV ($p<0.0001$)(Figure 1). Mean baseline BFV was negatively associated with periventricular WMH ($p<0.0001$) and normalized WMH volume ($p<0.0001$), uncontrolled DM as indicated by A1C ($p=0.01$), WBC ($p=0.05$), and intracellular adhesion molecule (sICAM-1) ($p=0.03$), and it was positively associated with baseline systolic BP ($p=0.004$) (whole model $R^2=0.86$ $p<0.0001$). This model controlled for the effects of age and BMI. C-reactive protein was negatively correlated with mean BFV ($p = 0.008$), but was positively associated with age ($p=0.01$), BMI ($p=0.003$), and WBC ($p=0.01$).

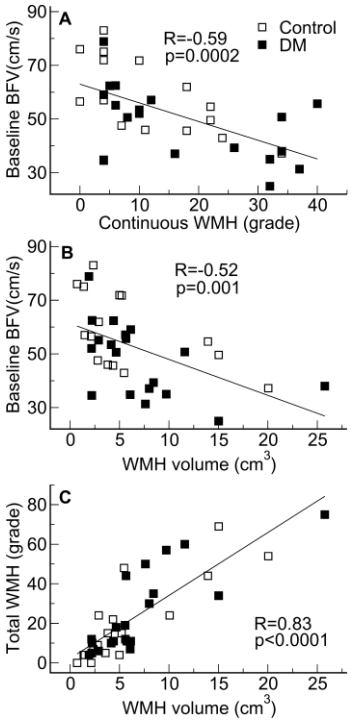

Figure 1: Relationship between baseline mean blood flow velocity (BFV) and sum grade of continuous white matter hyperintensity (WMH) on the visual rating scale (A) and WMH volume on MRI (B). Regression analysis revealed BFV significantly declined with increased WMH grade and volume. Regression analysis between the WMH volume on MRI and sum of continuous and punctuate WMH (total WMH grade) on the visual rating scale (C) for control (□) and DM (■) subjects.

Conclusions: Microvascular disease in type 2 DM that manifests as WM abnormalities on MRI is associated with reduced cerebral flow velocities and increased resistance. Inflammation may further contribute to reduced cerebral perfusion in older diabetic patients. These findings are clinically relevant as a potential mechanism for cerebrovascular disease in elderly persons with type 2 DM (**Appendix 1).**

C.2. Global and regional effects of type 2 diabetes mellitus on brain tissue volumes, cerebral blood flow, and CO_2 reactivity.

D. Last, D.C. Alsop, A.M. Abduljalil, R.P. Marquis, C. de Bazelaire, K. Hu, J. Cavallerano, V. Novak. Diabetes Care 2007;30:1193-99.

We examined the regional effects of type 2 DM on cerebral tissue volumes and blood flow regulation in 26 diabetic and 25 control subjects (aged 61.0 ± 7.5 years) using CASL MRI at 3 Tesla during baseline, hyperventilation, and CO_2 rebreathing. Regional gray matter (GM) and white matter (WM), cerebrospinal fluid (CSF), and WMH volumes (Figure 2) were quantified using segmentation method from T1-weighted inversion recovery fast gradient echo and FLAIR images at 3 Tesla MRI. The diabetic group had smaller WM ($p=0.006$) and GM ($p=0.001$) volumes and larger CSF volume ($p<0.0001$) than did the control group over the frontal, temporal, parieto-occipital, and cortical regions (Figure 2).

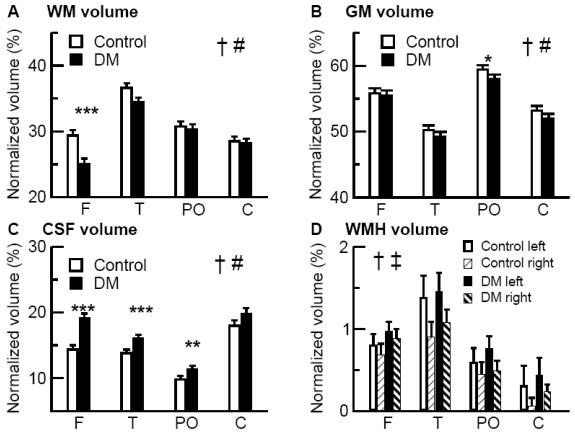

Figure 2: WM (A), GM (B), CSF (C), and WMH (D) volumes in the frontal (F), temporal (T), parieto-occipital (PO), and cortical (C) regions for both groups, normalized for region volume in control and DM groups (mean ± SE). † indicates between region comparisons for both groups $p < 0.0001$. ‡ indicates between hemispheres comparisons for both groups $p = 0.004$. # indicates between group comparisons over all regions $p \leq 0.006$. *** indicates between group comparisons within regions $p \leq 0.0008$, ** $p = 0.01$, * $p = 0.04$.

Regional CBF at baseline (p=0.006) and CO_2 reactivity were reduced (p=0.005) in the diabetic group (Figure 3). CBF reduction in the frontal region was associated with GM atrophy (p<0.0001). WMH volume affected CO_2 reactivity (p=0.0004) within the control group. Diabetic retinopathy was associated with greater CSF volume (p=0.001), in the temporal region (p=0.0003). Diabetes with hypertension was associated with increased CSF (p<0.0001) and decreased GM (p=0.008) volumes in the frontal (p<0.0001) and temporal (p=0.03) regions. In the DM group, A1C was associated with more atrophy (CSF: p=0.002) in the temporal region (p=0.02). **Conclusions**: Type 2 diabetes is associated with diminished cerebral blood flow and vasoreactivity and with cortical and subcortical atrophy affecting multiple brain regions. Associative areas of frontal and temporal cortices were most affected by diabetic metabolic disturbance and BP dysregulation (Appendix 1).

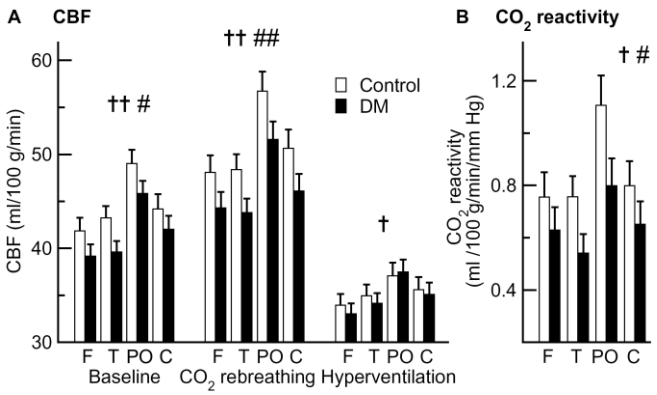

Figure 3: Cerebral blood flow (**A**) during the baseline, CO_2 rebreathing, and hyperventilation periods and the calculated CO_2 reactivity (**B**) in the frontal (F), temporal (T), parieto-occipital (PO), and cortical (C) regions in control and DM groups (mean ± SE). †† indicates between-region comparisons for both groups $p < 0.0001$, † $0.001 \le p \le 0.006$. ## indicates between-group comparisons over all regions $p = 0.001$, # $0.005 \le p \le 0.006$.

Registration of anatomical and perfusion images

We have further developed methodologies for MR image analysis and registration that allow direct comparisons between anatomical structures, perfusion (CASL), diffusion tensor (DTI) maps, and WMHs (see Methods section for details). **Figure 4** is an example of co-registration and normalization procedures of perfusion (CASL) and anatomical (MP-RAGE) and FLAIR images (1-5) and DTI images (6-7) for the subject with WMH grade 3 (A) and the control (B). The subject with WMHs on FLAIR images (A3) had lower perfusion in gray and white matter (A4, A5) than did the control subject (B3, B4). The WMHs areas are associated with abnormalities in diffusion and white matter integrity (A6, A7 vs. B6, B7). The volume and distribution of WMHs will be quantified on high resolution T2-weighted FLAIR images via thresholding of hyperintense pixels using a region growing method applied on WMH seeds. Excellent correlation for repeated measures of WMHs has been found with an intra-class correlation coefficient of 0.998 and inter-scan–coefficient of variation 4.8%, yielding a high reliability coefficient of 1.49 cm.[53]

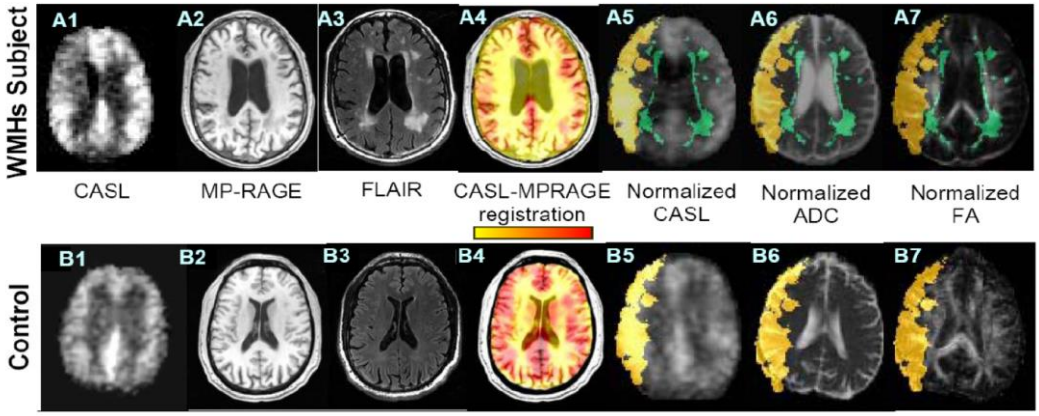

Figure 4: Example of perfusion and diffusion tensor image (DTI) registration on anatomical images for a subject with WMHs (A) and for a control (B). The perfusion CASL image (1) and the anatomical MP-RAGE image (2) are co-registered (4) and normalized to a standard template (5). Apparent diffusion coefficient (ADC) (6) and fractional anisotropy (FA) (7) maps derived from DTI are normalized to a standard template. The WMH regions (green) on the structural images (3) and MCA territory (yellow) are normalized and overlaid on normalized CASL (5), ADC (6), and FA images (7).

C.3. Autoregulation dynamics assessed by multi-modal pressure-flow method (MMPF).
K. Hu, C.K. Peng, V. Novak et al. J. Cardiovasc Eng, In press) and K. Hu, C.K. Peng, V. Novak et al. American Journal of Physiology, Currently under Review).

Cerebral autoregulation reflects the ability of microvasculature to adapt to systemic BP variations and metabolic demands. The MMPF analysis implements the Hilbert-Huang transformation[54] to measure the coupling between two nonstationary signals. MMPF analysis decomposes complex BP and BFV signals into multiple empirical modes, representing their instantaneous frequency-amplitude modulation. The MMPF method, which does not make any assumptions about linearity or stationarity of the signals, is ideally suited for the analysis of the short nonstationary time-series during interventions such as the Valsalva maneuver. Development of MMPF was motivated by the fact that the cerebral BFV signals are recorded with peripheral BP over time. However, different subjects vary in the amount of time spent in each stage of the intervention. Therefore, it is essential to find an alternative coordinate system for both BP and BFV signals that allows for a meaningful, non-time-dependent cross referencing of these two signals. Spontaneous fluctuations in cerebral BFVs reflect dynamics of adaptation to intracranial pressure and systemic BP changes. MMPF is a novel approach for assessment of autoregulation dynamics that has been recently validated in patients with hypertension and stroke during the Valsalva maneuver[55] and using spontaneous BP fluctuations. Figure 5 shows comparisons of MMPF estimates of autoregulation between the spontaneous oscillations and those with the Valsalva maneuver.

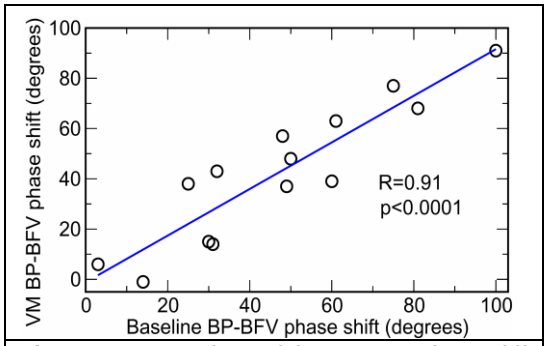

Figure 5: Comparison of the BP-BFV phase shift at the BP minimum during two different conditions. For each subject in this study, BP-BFV phase shifts were measured during Valsalva maneuver and spontaneous BP oscillations during supine rest. These two measurements show a strong correlation, as indicted by linear regression fit (R=0.91).

The BP-BFV phase shift during spontaneous fluctuations were examined in 20 control (aged 56.2 ± 12.1 years) and 20 DM subjects (aged 61.0 ± 7.2 years) during a 5-minute supine rest. Figure 6 shows dominant spontaneous oscillations of BP and BFV in (**A**) a control and (**B**) diabetic subjects. BP and BFV signals were decomposed into different modes using an ensemble empirical mode decomposition algorithm, each mode corresponding to fluctuations at different time scale. BP and BFV fluctuations exhibit continuous and dominant oscillations at the frequency from ~0.07 to 0.4 Hz. The dominant oscillations were extracted and used for the assessment of the BP-BFV relationship. Instantaneous phases of BP and BFV oscillations were obtained using the Hilbert transform. The instantaneous BP-BFV phase shifts were averaged **(C)** and compared between the groups. BP-BFV phase shifts reflecting spontaneous dominant oscillations were much smaller in the diabetes group than in the healthy control group (p<0.0001) for both MCAs. Multiple regression analysis did not show any additional effects of hypertension or retinopathy on the observed group differences in BP-BFV phase shifts. Traditional estimates of autoregulation did not reveal group differences. **Conclusions:** These results suggest that diabetes slows down vasoregulation and that perfusion pressure follows fluctuations in systemic BP (**Appendix 1).**

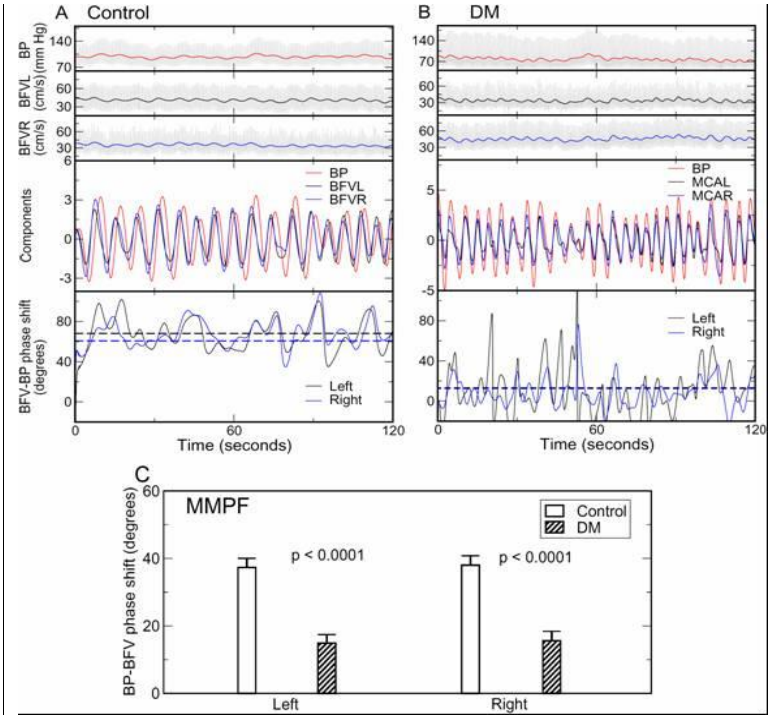

Figure 6: Dominant spontaneous oscillations of BP and right and left BFV in (A) a control and (B) a DM subject during supine baseline (panels 1-3). Dominant oscillations at the frequency from ~0.07 to 0.4 Hz (panel 4). Instantaneous phases of BP and BFV oscillations(panel 5). (C) The average of instantaneous BP-BFV phase shifts for all cycles of dominant oscillations for DM and control groups (mean±SE).

C.4. Effects of high body mass index on cerebral blood flow.
M. Selim, R. Jones, P. Novak, V. Novak. Currently under review, Int. J. of Obesity.
Obesity is a risk factor for cerebrovascular disease. We aimed to determine the effects of high body mass index (BMI) on cerebral blood flow regulation in patients with type 2 DM, hypertension, or stroke. This study was cross-sectional analysis. We analyzed data from 90 controls, 30 diabetics, 45 hypertensives, and 32 ischemic stroke patients who underwent TCD for evaluation of BFVs in the MCAs and cerebrovascular resistance (CVR) during supine rest and head-up tilt. We used a structural equation multiple indicators modeling to determine the effects of BMI and other background variables (age, sex, race, smoking, alcohol use, and systolic BP) on cerebral BFVs. Higher BMI (p=0.02) and age (p=0.004) were associated with lower mean BFVs during baseline, independent of diagnosis and after adjusting for all background variables (Figure 7). Diabetic subjects had lower BFVs than did controls (p=0.017). Men, especially those with stroke, had a lower mean BFV than women (p=0.01). CVR increased with BMI (p=0.001) at baseline and during head-up tilt (p=0.02), and was higher in obese subjects (p=0.004) than in normal weight subjects across all groups. **Conclusions:** High BMI is associated with a reduction in cerebral BFV and increased CVR. These findings indicate that obesity can adversely affect cerebral blood flow and resistance in the cerebrovascular bed, independent of diagnosis of type 2 diabetes, hypertension, or stroke. Obesity may contribute to cerebromicrovascular disease and affect clinical functional outcomes of an older population.

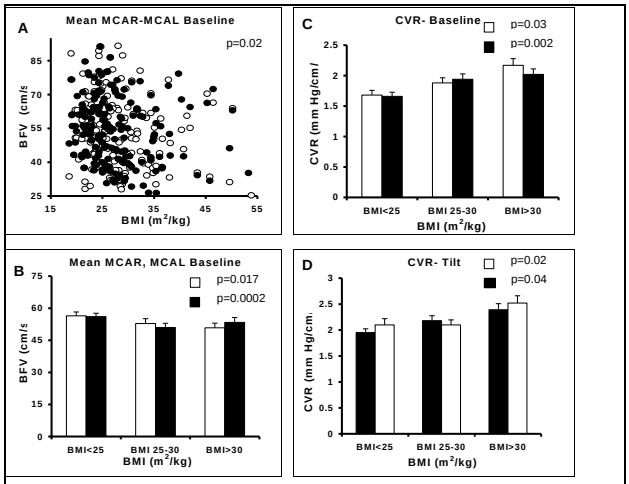

Figure 7: Panels A and B show the relationship between body mass index (BMI) and age-adjusted mean blood flow velocities in right and left middle cerebral artery (white- MCAR, black-MCAL) during baseline in all groups. Panels C and D show the average cerebrovascular resistance (CVR in MCAR and MCAL during baseline and head-up tilt (mean± SE).

In our Aim 3 we plan to determine prospectively the relationship between diabetes, brain atrophy, and functional outcomes of cognition and balance that we support with our cross-sectional studies described below in sections (C.5-C.8).

C.5. Cognitive dysfunction is associated with poor diabetes control in older adults.
M. Munshi, L. Grande, M. Hayes, et al. Diabetes Care 2006; 29:1794-9.
The objective of this study was to evaluate the association between cognitive decline, other barriers to treatment compliance, and glycemic control in older adults with DM. Patients aged >70 years presenting to a geriatric diabetes clinic were evaluated for barriers to successful diabetes management. Patients were screened for cognitive dysfunction with the mini mental status examination (MMSE) and a clock drawing test (CDT) scored by 1) a method validated by Mendez et al. and 2) a modified clock box drawing test (clock-in-a box [CIB]). Depression was evaluated with the geriatric depression scale (GDS). Interview questionnaires surveyed activities of daily living (ADLs) and instrumental ADLs (IADLs), as well as other functional disabilities. Sixty patients (aged 79 $\pm$ 5 years; duration of diabetes 14 $\pm$ 13 years; A1C 7.9 $\pm$ 1.4%) were evaluated. Thirty-four percent had a low CIB score of $\leq$5 and CDT $\leq$ 13),.and A1C >8%. Both CIB and CDT were inversely correlated with A1C, suggesting that cognitive dysfunction is associated with poor glycemic control (r=-0.37, p <0.0004 and r=-0.38 p <0.004, respectively). Thirty-three percent of patients had depressive symptoms with greater difficulty completing the tasks of the IADL survey (5.7 $\pm$ 1.7 vs. 4.6 $\pm$ 2.0; p <0.03). These older adults with diabetes had a high incidence of functional disabilities, including hearing impairment (48%), vision impairment (53%), history of recent falls (33%), fear of falls (44%), and difficulty performing IADLs (39%). **Conclusions**: Older adults with diabetes have a high risk of undiagnosed cognitive dysfunction, depression, and functional disabilities. Cognitive dysfunction in this population was associated with poor diabetes control **(Appendix 1)**.

C.6. Effect of blood pressure and diabetes mellitus on cognitive and physical functions in older adults: a longitudinal analysis of the advanced cognitive training for independent and vital elderly cohort.

H.K. Kuo, R.N. Jones, W. Milberg, et al. J. Am.Geriatric. Soc. 2005;53:1154-61.

This study evaluated the effect of BP and DM on cognitive and physical performance in older, independent-living adults. This was a longitudinal study with secondary data analysis from the Advanced Cognitive Training for Independent and Vital Elderly randomized intervention trial in six field sites in the U.S., enrolling 2,802 independent-living subjects aged 65 to 94. Cognitive functions in different domains and physical functions measured using activities of daily living (ADLS, IADLs), and the physical function subscale from the Medical Outcomes Study Short Form-36 (SF-36) Health Survey. After the first annual examination, hypertension was associated with a faster decline in performance on logical reasoning tasks (ability to solve problems following a serial pattern), whereas DM was associated with accelerated decline on the Digit Symbol Substitution Test (speed of processing). The reasoning and Digit Symbol Substitution Test are executive function tasks thought to be related to frontal-lobe function. Hypertension and DM were associated with a significantly faster pace of decline on the SF-36 physical function component score. Individuals with DM had a faster pace of decline in IADL functioning than did non-diabetic subjects. There was no evidence for an interaction between BP and DM on cognitive or physical function decline. **Conclusions:** Hypertension and DM are associated with accelerated decline in executive measures and physical function in independent-living elderly subjects.

C.7. White matter hyperintensities and dynamic postural control.

V. Novak, M. Haertle, K. Hu, et al. J. Gerontology. Currently under Review.

We have determined the relationship between WMHs on MRI and blood flow velocities (BFV) in MCA and the relationship between WMHs and balance in 55 healthy normotensive (NTN), 21 normotensive DM (DM-NTN), 14 hypertensive DM (DM-HTN) and 14 non-diabetic hypertensive (HTN) subjects. WMHs were graded and their volume was quantified from FLAIR images at 3 Tesla MRI. To assess balance, center of pressure (COP) displacement was measured using the force platform during 3-min quiet standing with eyes open or closed. COP data were analyzed using traditional posturographic parameters and dynamic measures based on stabilogram-diffusion analysis including short-term positive correlation based on Hurst exponent (h) (in mediolateral and anteroposterior direction (hxs, hys), long-term negative correlation (hxl, hyl), transition time between two domain in both directions (nx, ny) and fluctuation amplitudes (RMSx, RMSy) of transition from positive to negative correlations. All data were adjusted for age and for brain size. Control subjects had less total brain continuous and punctuate WMHs (p=0.006 and p=0.04) and smaller WMHs volume. DM-HTN and HTN groups had more continuous WMHs (p=0.004 and p=0.002) and punctuate WMHs (p=0.05 and p=0.005) and greater WMH volumes than controls (p=0.0064). The HTN group had more punctuate WMHs (p=0.016). The DM-NTN group was not different from controls. **Balance control:** No significant differences were found in traditional posturographic measures. **Regression analysis WMHs and balance control:** Continuous and punctuate WMHs were associated with larger long-term medio-lateral fluctuations (hxl_1, p=0.0001 and p=0.002) and shorter transition time (nx_1 p=0.0003 and p=0.023) and nx_2 (p=0.016 and 0.013). WMH volume was associated negatively with short-term mediolateral fluctuations (hxs_1 (p=0.023) that had smaller amplitude (RMSx_1 (p=0.032) and with larger anteroposterior long-term fluctuations (hys_1 p=0.019). Diabetes, particularly diabetes with hypertension, increases severity of microvascular disease and affects the dynamics of balance control.

D. RESEARCH DESIGN AND METHODS

Overview

This single-center study aimed to determine prospectively the impact of type 2 diabetes on brain tissue damage and its consequences for cognition and balance in older adults. The motivation here is that type 2 DM is associated with microvascular disease that may affect cerebral perfusion, cognition and balance and that poor glycemic control further accelerates brain atrophy and functional decline. For Aim 1, we used a structure-function approach that combines anatomical and functional MR-CASL perfusion imaging. For Aim 2, we determined the effects of inflammation on white matter integrity by using diffusion tensor imaging. For Aim 3, we prospectively followed our cohort of diabetic and control subjects over a 2-year period to determine relationships between neuroanatomical changes and functional decline in cognition and balance. We also determined whether higher levels of A1C are associated with a greater decline in perfusion and worse outcomes. Our analytical approach allowed us to detect interactions and causal relationships between diabetes, structural brain changes, perfusion, and outcome measures. The results of this study may provide new biomarkers of diabetic metabolic disturbance in the brain that can be used to predict cerebrovascular complications of diabetes.

Subject Selection Criteria

Inclusion criteria—diabetes group. This group consisted of 60 men and women aged 50-85 years diagnosed with type 2 DM and treated >5 years with oral agents and/or combinations with insulin, either normotensive (BP <140/90 mm Hg and no medical history of hypertension) or hypertensive (BP >140/90 mm Hg and/or treated for hypertension). Diabetes severity was assessed from diabetes duration, hemoglobin A1C, and fasting glucose levels, and from microvascular and macrovascular complications.[1] "Any microvascular disease" is defined as diabetic retinopathy, albuminuria, neuropathy, or incidental lacunar infarct [1) diabetic retinopathy (defined as score >1.0 on retinal images evaluated via the Joslin Vision Network using nonmydriatic digital retinal imaging protocol [2,3,4,5,6,7]; 2) albuminuria (defined as microalbuminuria albumin 30-250 mg/L and macroalbuminuria albumin >250 mg/L); 3) peripheral neuropathy (score >6 on Toronto neuropathy scale)[8,9]; 4) lacunar infarct (by radiological criteria on T2-weighted MRI]. "Any macrovascular disease" is defined as a history of myocardial infarction or surgery or endovascular treatment for coronary, carotid, or peripheral (legs, abdominal aorta) disease.

Inclusion criteria—control group. This group consisted of 60 men and women matched with the diabetes group by age ±5 years, sex, and hypertension (normotensive [BP <140/90 mm Hg and no medical history of hypertension] and hypertensive [BP >140/90 mm Hg and/or treated for hypertension]). The control group had normal fasting blood glucose and A1C and normal cognitive function (MMSE). If a control subject's total MMSE score is $\geq$3 points below the Comparative Normal Value for the subject's age group and education level, or $\leq$ 24, he or she was excluded from participation in the study.

Exclusion criteria. Persons with any one of the following conditions were excluded: type I diabetes, any unstable or acute medical condition, myocardial infarction or major surgery within 6 months, history of a major stroke, dementia (by history) or inability to follow details of the protocol, carotid stenosis > 50% by medical history, Doppler ultrasound, or MR angiography; hemodynamically significant valvular disease; arrhythmias, liver or renal failure or transplant; severe hypertension (systolic BP >200 and/or diastolic BP >110 mm Hg or subjects taking $\geq$3 antihypertensive medications); seizure disorders; malignant tumors, current recreational drug or alcohol abuse; active smoking; morbid obesity (BMI >40); inability to obtain permission for participation from the primary care physician. Women in both groups were required to be postmenopausal. MRI exclusion criteria include any metallic bioimplants (including pacemakers and valve replacements not compatible with 3 Tesla MRI guidelines), claustrophobia, or inability to cooperate. TCD exclusion criteria – poor insonation window and TCD signal.

Recruitment. Diabetic subjects were recruited from the Joslin Diabetes Clinic and the Geriatric Diabetes Clinic at the BIDMC, where 300 patients aged >70 years are followed and more than 125 new patients are seen each year. The SAFE Laboratory database, family members, and advertisements were used for recruitment of non-diabetic participants. The enrollment goals were based on our cross-sectional DM trial, in which 55 subjects completed 3 visits (tilt table testing, TCD, and MRI), and 6 subjects (8.6%) who dropped out. We anticipated that we would screen 280 subjects by phone, obtain signed consent forms from 180 subjects, and complete the first study visit in 140 subjects (accounting for an anticipated drop-out of 17% subjects) to meet our enrollment goals of 120 subjects upon the trial's completion over a 2-year period.

Protocol Overview

Studies were conducted in the SAFE Laboratory at the BIDMC GCRC and at the Center for Advanced Magnetic Resonance Imaging, Department of Radiology at the BIDMC. The experimental protocol described below is feasible in elderly people, and admission to the GCRC allows for continuous medical supervision. The protocol time line and safety procedures are detailed below (**Table 1**) and in the Human Subjects section. The Principal Investigator has extensive experience in transcranial and carotid Doppler ultrasonography and in autonomic function testing in the elderly, which she obtained during her training at the Mayo Clinic, as the Director of Autonomic System Laboratory at The Ohio State University, and as the Director of SAFE Laboratory at the BIDMC.

Table 1: Protocol Time Line

Visit	**Procedures**
Screening	Hx, ECG,TCD window, blood draw, MMSE, physician permission,
BP taper	Home BP monitoring 4× per day, for 3 days, BP&DM meds on
Visit 1	**Day 1-**
	Admission to GCRC, neuroexam, cognitive testing, retinal imaging, anthrop. meas., BP&DM meds on
	Day 2
	Fasting labs, TCD study, balance study, MRI, BP meds off, DM on
Follow-up 6, 12, 18 mo.	Fasting glucose, A1C, blood panel, BP, meds and Hx update, vital signs, anthrop.meas.
Visit 2 24 months	**Day 1 and Day 2** same procedures as visit 1

Subjects' screening and pre-tests. All subjects who were interested in this study and met inclusion/exclusion criteria were invited to the BIDMC GCRC and asked to read and sign the informed consent. They were asked to fill out a medical history and autonomic symptoms and activity questionnaires. A GCRC nurse obtained ECG, vital signs, height, and weight. Blood was drawn to obtain glucose and renal panels, A1C, lipid profile, hematocrit, CBC, and WBC. Insonation window for TCD were assessed. Heart rate and BP were measured during sitting and after 1, 3, and 5 minutes of standing. MMSE was used for cognitive function screening. Each subject's primary physician was contacted for pertinent medical information, their opinion regarding the subject's compliance, and their approval for participation.

Protocol flow sheet

BP medications taper. To establish BP baseline, BP was monitored for 3 days while the subject was taking their usual dose of antihypertensive medications. BP was monitored 4 times a day at home. Antihypertensive medications were held on Day 2 of the study.

Visit 1 schedule: **Day 1 (Table 1).** Subjects enrolled in the DM and control groups were admitted to BIDMC GCRC. Study physicians performed physical and neurological exams and neuropathy assessments. Ophthalmologic examination was done at the Beetham Eye Institute at the Joslin Diabetes Center using the Joslin Vision Network (JVN). Cognitive testing battery was done. A GCRC-trained nurse measureed vital signs, as well as anthropometric and **adiposity measures** using skin fold thickness (SKF) and waist-to-hip ratio. We added SKF and waist-to-hip ratio as our measures of adiposity and body fat distribution. SKF is a noninvasive technique that has been shown to correlate with DEXA scans (r=0.94) and bioelectrical impedance (r=0.91)[10].

Day 2. Blood was drawn to obtain fasting glucose, A1C, C-peptide, lipids, hematocrit, WBC, C-reactive protein (CRP), intracellular adhesion molecule-1 (sICAM-1), vascular adhesion molecule (sVCAM-1), tumor necrosis factor (TNF-α), and interleukin 1-6 (IL1-6), and blood and urine samples were used for renal panels. TCD and MRI studies proceeded according to the protocol described in the Methods section. Glucose control medications were not modified, but antihypertensive medications were held on morning Day 2 and restarted upon the completion of hemodynamic studies at the usual dose before discharge from GCRC.

Follow-up visit. All subjects were invited to BIDMC every 6 months for a follow-up visit that included measurements of fasting glucose, A1C, blood and urine panels, vital signs, anthropometric and body fat measures, and updates on medical history and medications.

Visit 2: 2-year follow up
The protocol for the 2-year follow up visit is the same as for the first visit (**Table 1**).
We describe below the details of experimental protocol, computational procedures, and statistical analyses; **Table 2** summarizes the variables, measures, and instruments used for analyses of these Aims.

Table 2: Summary of variables and instruments for analyses

Category	Measure	Source of Information	Discrete Score	Continuous Variables
Independent variables				
Demographic	Age, sex, adiposity,	Skinfold thickness Waist-to-hip ratio	M/F	Age, adiposity
Diabetes severity	A1C, DM duration, fasting glucose	Laboratory values		A1C, glucose values, DM duration (yrs)
Cardiovascular risk	Microvascular: retinopathy albuminuria, neuropathy Macrovascular: CVD, MI, CAD, PVD, cholesterol, lipids, hypertension	Medical history	Each factor present/absent	Serum values, BP values, HTN duration (yrs)
Blood tests	Inflammatory markers: WBC, CRP, sICAM-1, sVCAM-1, TNFα, IL6, IL10	Assay		Serum values
Dependent variables				
MRI	Brain volume	T1, T2, FLAIR, MP-RAGE, segmentation		Regional GM, WM, CSF volumes; WMHs fractional anisotrophy
	Blood flow	CASL MRI		Regional perfusion
Vasoreactivity	CO_2 Pressure autoregulation Cognitive challenge	CASL MRI TCD		Regional perfusion and reactivity maps Slope of regression Flow/CO_2 BP-BFV phase shift
Cognitive Function	Executive Function.	Trail Making test A,B Verbal fluency	Median cut-off	Individual scores
	Memory Function	Logical Memory Boston Naming Digit Span Rey Figure	Median cut-off	Individual scores
Balance	Balance	Force displacement		COP Short-term and long-term and cross-over diffusion coefficient

Methods for Specific Aim 1 In Aim 1 we planned to determine the effects of type 2 DM on (a) regional cerebral volumes and perfusion and (b) the dynamics of cerebral vasoregulation.

Aim 1a. To determine the effects of type 2 DM on regional gray and white matter and cerebrospinal fluid volumes and on perfusion maps in diabetes and control groups.

Experimental protocol for MRI studies

Studies were done in the Magnetic Resonance Imaging Center at the BIDMC in the 3 Tesla, GE Vhi scanner with quadrature head coil. Standard safety procedures were implemented. A mask placed on the subject's face was connected to the CO_2 rebreathing circuit, and CO_2 and vital signs were measured. MRI techniques for the CBF and anatomical imaging and signal processing methods we proposed have been established in our center.

T1- and T2-weighted imaging. High-resolution anatomical images from all subjects were acquired with the following parameters: 3D T1- weighted inversion recovery fast gradient echo (IR-FGE): T_I = 600 ms, T_E/T_R = 3.3/8.1 ms, flip angle of 10 degrees, 3 mm slice thickness, 24 cm × 19 cm Field of View (FOV), 256 × 192 matrix size; fluid-attenuation inversion recovery (FLAIR): T_I = 2250 ms, T_E/T_R = 161/11000 ms, 5 mm slice thickness (0 mm slice spacing), 24 cm × 24 cm FOV, 256 × 160 matrix size; dual T2-weighted fast spin echo (FSE): T_E = 25/117 ms, T_R = 4000 ms, 3 mm slice thickness, 24 cm × 18 cm FOV, 256 × 256 matrix size; 3D-MR angiography (time of flight, TOF): T_E/T_R = 3.9/38 ms, flip angle of 25 degrees, 2 mm slice thickness, 20 cm × 18 cm FOV, 384 × 224 matrix size. Diffusion tensor imaging (DTI): T_E = 112 ms, TR = 10000 ms, 24 cm × 24 cm FOV, 5 mm slice thickness, 0 mm slice spacing, 30 slices 4:40,128 x 128 matrix, 1 NEX, bandwidth = 167 Khz, B value = 1000, diffusion = 25 tensor directions. Positioning scan was recorded and scanner stability was measured using routine phantom procedures for scanner stability.

Cerebral blood flow and reactivity measurements. CASL at 3 Tesla MRI was used to measure regional distribution of perfusion during baseline rest and flow reactivity to CO_2 and cognitive challenges. Two baseline blood flow measurements were taken during normocapnia. Subjects hyperventilated to reduce CO_2 to 25 mm Hg for 2 minutes. Subjects equilibrated CO_2 during supine rest. Then subjects breathed a mixture of 5% CO_2 and 95% air from the rebreathing bag to increase CO_2 above baseline to 45 mm Hg for 2 minutes. Subjects equilibrated CO_2 during supine rest. During cognitive challenges, subjects were asked to subtract odd numbers (7, 13, or 17 in random order) from the number 300 over 2 minutes. Blood pressure were measured at 1-minute intervals.

Data processing and image analysis for MRI studies Aim 1a

Primary end points are regional gray and white matter and cerebrospinal fluid matter volumes in diabetes and control groups. Secondary end points are regional perfusion and vasoreactivity to CO_2 and cognitive challenges in gray and white matter. **Table 2** summarizes the dependent and independent variables for Aim 1.

Image segmentation and registration

Evaluation of the relationships between blood flow alterations and structural abnormalities in the brain and their impact on functional outcomes required a within-subject inter-modal "registration" (alignment) between structural and perfusion images that has been implemented in our laboratory, as illustrated in the Preliminary Results section (see Figure 4). T1-weighted MP-RAGE images were employed to assess volume of CSF and white and gray matter, according to the anatomical lobes and in basal ganglia. White matter integrity and WMHs were evaluated on DTI and FLAIR images. A rigid-body model[56,57] was used for registration of MP-RAGE image on DWI, FLAIR, and CASL images using the Statistical Parametric Mapping software package (SPM, Wellcome Department of Imaging Neuroscience, University College London, UK). The 'normalization' module in SPM is employed to stereotactically normalize structural images to a standard space defined by some ideal template image(s), by matching gray matter in these images to gray matter in a reference image using rigid-body transformation and 3–D rotation. Since the normalization transformation can also be applied to any other image that has been registered with these scans, the aligned perfusion images were normalized to standard space by the same transformation.[58] The registered MP-RAGE image was segmented into CSF, GM, and WM by an inherently circular model in SPM involving spatial normalization and tissue classification.[59] Segmentation of WMHs on FLAIR image was programmed in Interactive Data Language (IDL, ITT Visual Information Solutions). Regions of interest containing WMHs on FLAIR images were outlined and their seeds were identified using the thresholding of hyperintense pixels. The borders were detected using a region growing method applied on WMHs seeds. To measure CBF in anatomical regions of interest and surrounding tissue, perfusion maps were registered on the anatomical images to achieve automatic selection of these regions of interest. Cerebral blood flow maps

were created and CBF was normalized for tissue volume and quantified as (mL / 100 g / min). The rigid-body model was used again for registration of the perfusion image on the structural image, and then the registered perfusion image is overlaid on the segmented anatomical regions and WMHs to achieve the CBF in these regions. The registration was completed by appropriate weighting of the template voxels. This is an automated procedure, which discounted the confounding effects of skull and scalp differences. A Bayesian framework was used, such that the registration searches for the solution and maximizes the a posteriori probability of its being correct, i.e., it maximizes the product of the likelihood function (derived from the residual squared difference) and the prior function (which is based on the probability of obtaining a particular set of zooms and shear). The affine registration was followed by estimating nonlinear deformations wherein the deformations are defined by a linear combination of three-dimensional discrete cosine transform basis functions. General methods and intrasubject, intramodality validation were used for this step. This iterative algorithm estimated the best parameter values of a given 3D spatial transformation model that would yield the best match between the reference image and the image to be registered. This was achieved by minimizing a given cost function. Eventually, the spatial transformation with the lowest cost function value was selected and used to compute the registered image.

Segmentation of white matter hyperintensities

The volume and distribution of WMHs were quantified on high resolution T2-weighted FLAIR. On the FLAIR ROI, WMHs seeds were identified via thresholding of hyperintense pixels using a region growing method applied on WMHs seeds. Periventricular WMHs are described as ill-defined and moderately hypodense (>30% signal intensity change) areas of ≥5 mm on T2-weighted images. Lacunes are well-defined areas of >2 mm with signal characteristics the same as CSF.[60] The EM algorithm converges when changes in the estimations are less than a given threshold value and the final estimates are obtained. Segmentation masks were created and WMH areas were calculated for each segmentation mask for each image. The WMH volume were derived from reconstructed 3D images. Excellent correlation for repeated measures of WMHs has been found with an intra-class correlation coefficient of 0.998 and an inter-scan–coefficient of variation of 4.8%, yielding a high reliability coefficient of 1.49 cm.[53] Our preliminary data showed an excellent correlation between the visual rating scale and WMH volume measurement (coefficient of correlation 0.83).[47]

Cerebral blood flow mapping using CASL MRI

3D continuous arterial spin labeling (CASL) at 3 Tesla MRI was used to measure regional distribution of CBF and cerebral vasoreactivity. 3D CASL that allows CBF mapping [61] was been implemented for 3 Tesla MRI. With this technique, labeling of inflowing arterial water is achieved by the application of optimized time varying magnetic fields. The naturally occurring hydrogen nuclei of water become the label which then decays with the MR longitudinal relaxation time T1 (approx. 1.4 seconds in blood). A labeled image was subtracted from an unlabeled image to measure CBF. Measurement of the tissue-dependent T1 and use of established theory[62,63] permit the calculation of absolute blood flow into tissue.[64] CASL was done as previously described.[65,66,67] Echoplanar T1 mapping scans was used for image registration and for the correction of spatial distortion of the images by static magnetic field in-homogeneities. A scout image of the head was obtained in order to choose the appropriate location for spin labeling and flow imaging. 3D CASL images were acquired using 3D gradient echo-planar images (T_E = 5 ms, FOV = 24 cm × 24 cm, slab thickness = 15.2 cm, matrix size: 128×128×40, bandwidth = 62.5 kHz) over 2 minutes. Typically, these images were averaged during baseline, hyperventilation, CO_2 rebreathing, and cognitive challenge (2 minutes for each session) in order to improve the signal-to-noise ratio. Finally, a regional T1-weighted map was obtained using a modification of the spin labeling sequence. All image data were loaded on a Linux workstation for subsequent analysis using tools developed in the IDL programming environment (Research Systems, Boulder, CO). Quantitative CBF images were calculated as previously described.[65] Cerebral vasoreactivity maps were derived from perfusion images as the difference between percentage of flow augmentation during CO_2 rebreathing and flow reduction during hyperventilation, divided by CO_2 change. Perfusion difference between baseline and responses to cognitive challenge were be calculated by subtracting the images. Additional smoothing in 3 dimensions could be employed, if needed, to correct movement artifacts not eliminated by the algorithm for motion-correction. All perfusion values will be converted to mL/100g/min units.

Diffusion tensor imaging

Diffusion tensor imaging (DTI) was implemented to study the initial diffusion weighted abnormality and to calculate the volume of acute lesion on the apparent diffusion coefficient (ADC) maps in acute stroke. DTI provides a contrast based on the water molecules' diffusion and its direction. This contrast is influenced by the tissue structure and can be used to indicate changes in its integrity. Ultrastructural changes in diffusivity in WM will be quantified using an ADC coefficient and fractional anisotropy (FA) that will be used to measure directionality of diffusion along WM pathways.[68,69] ADC and FA will be calculated in the regions that demonstrate WMHs on DWI, as shown on Figure 4 (A7, B7) in the Preliminary Results section. The diffusion can be modeled using a symmetric second order tensor. By diagonalizing the diffusion tensor, one can obtain the orthogonal principal axes where the water molecules' displacement is uncorrelated. The corresponding eigenvalues λ_1, λ_2, and λ_3 are normally arranged in a decreasing order, and their values represent the probability of displacement in the related direction.[70] The microstructure of the WM and the restrictive nature of the myelin membrane create a preferred displacement direction along the neural fiber. A good measure that quantifies this preference is the fractional anisotropy, defined as $FA = \sqrt{3 * \sum_{i=1,2,3} \left(\lambda_i - \lambda_{avg}\right)^2} \Big/ \sqrt{2 * \sum_{i=1,2,3} \lambda_i^2}$, where λ_{avg}, is the average value of the eigenvalues. Any decline in fractional anisotropy indicates a neural degeneration and demyelination. Age-related changes in the WM can cause a regional decline in anisotropy, namely, the frontal WM, the posterior limb of the internal capsule, and the genu of the corpus callosum.[68]

First, 30 slices covering the whole brain were acquired, and this step was then be repeated 26 times, each with a different value of diffusion gradient pulses. The acquired images were corrected initially for motion as well as image distortions, followed by the calculation of the diffusion tensor matrix for every voxel. The FA was evaluated from the tensor matrix. The corrections and calculations were performed using the Guided Tensor Restore Anatomical Connectivity Tractography (GTRACT) tool.[71] Finally, the calculated maps were co-registered on the high resolution MP-RAGE images where a 12-parameter affine transformation were achieved using FRIB software library tools.[72]

Statistical analysis for MRI data - Aim 1a

A complete dataset for each patient included CASL, DTI, T1- and T2-weighted MP-RAGE and FLAIR images, and CO_2 VR maps during visit 1 and the follow-up visit 2. Brain tissue volumes, CSF**,** CBF, and CO_2 and cognition task reactivity were quantified for anatomical regions of interest, frontal, temporal, and parieto-occipital lobes, hippocampus, cingulum and mesiotemporal lobes. The first end point is the regional volume of gray and white matter and CSF in the DM and control groups as determined using the segmentation method. The second end point is CBF in gray and white matter in the DM and control groups. Cerebral blood flow maps were created and CBF was normalized for tissue volume and quantified as (mL / 100 g / min).[67] CBF in each region and in gray and white matter, respectively, was summarized using descriptive statistics. Baseline CBF between the DM and the control group were compared using the multivariate mixed models, adjusting for the effects of regions, right and left hemisphere, age, sex, A1C, and DM duration. The effects of adiposity, hypertension and co-morbidities and their interactions were explored separately. The CO_2 reactivity was computed in each region as the slope of the linear fit between CO_2 and CBF values among baseline, hypocapnia, and hypercapnia using same approach. The response to cognitive challenge was calculated as percentage CBF augmentation between baseline and cognitive testing for each region and analyzed using the same approach.

Power for MRI data - Aim 1a

Based on our preliminary data, with 60 DM and 60 control subjects we aimed to have 99% power to detect 5.3% difference in normalized CSF volume in the frontal region (control 14.3 $\pm$ 4.0 vs. DM 19.6 $\pm$ 5.0%) and 99% power to detect 4% difference in WM volume (29.0 $\pm$ 6.0 vs. 25.0 $\pm$ 4.0%) using two-sample t-test, alpha 0.05. We aimed for 99% power to detect a difference of 2.3 mL/100 g/min in the baseline regional CBF (baseline CBF in frontal region for the control 42.5 $\pm$ 1.3 vs. DM 38.6 $\pm$ 1.2 for a difference of 3.9, and in temporal region for the control 43.8 $\pm$ 12.0 vs. DM 39.2 $\pm$ 1.1 groups for a difference of 4.6 mL/100 g/min) using two-sample t-test, alpha = 0.05, based on our preliminary data. For CO_2 reactivity we had 99% power to detect a difference of reactivity 0.1 mL/100 g/min/mm Hg within a region, based on differences in vasoreactivity in temporal region values in control 0.68 $\pm$ 0.08 vs. DM 0.61 $\pm$ 0.08 mL/100 g/min/mm Hg. Generally speaking, a sample size of 60 DM and 60 controls were provided sufficient power to detect differences in normally distributed outcomes that are 0.633

standard deviation units or greater as statistically different from zero. Such effects fit with what Cohen[11] classified as a medium to large effect size. Similarly, conventional rules of thumb on the number of variables to include in a model limited the complexity of our models to no more than 12 variables. However, we felt that certain aspects of our design mitigate this risk of low power. First, our design employed rigid eligibility criteria and attenuates random variability in the systems we are studying, thereby lowering standard deviations and increasing effect sizes likely to be detected. Second, our approach made use of data reduction activities and generated composites that collapsed multiple indicators of complex traits (e.g., metabolic syndrome) into single variables. For multivariate analyses such as factor analysis, a sample size of 120 is often considered poor to fair.[73] To account for this, we used analysis models derived from Rasch [74] that avoided estimating slopes (factor loadings). This was accomplished by fitting factor analysis models assuming equality of factor loadings. We evaluated model residuals for evidence of mis-fit to relax assumptions or modify the inclusion of specific indicators.

Aim 1b: To determine the effects of type 2 DM on the dynamics of cerebral vasoregulation.

The effects of DM on the dynamics of cerebral vasoregulation was determined from changes in blood flow velocities (BFVs) in the anterior and middle cerebral arteries (ACA and MCA) determined using TCD during hypocapnia and hypercapnia and from changes in blood pressure induced by head-up tilt.

Experimental protocol for ultrasound TCD studies

Instrumentation for measurements of heart rate, BP, BFV, respiration, and CO_2 will take about 30 minutes. Heart rate was measured using a 3-lead electrocardiogram. Beat-to-beat arterial pressure *was* measured from a cuff placed on the finger using a Portapress-2 device (FMS, Inc). Beat-to-beat BP measurements were initially corroborated by standard measurements of arterial pressure on the upper arm (Dynamap). Respiratory rate, tidal volume, and end-tidal CO_2 values were measured, using an infrared end-tidal volume gas monitor (Capnomac Ultima, Ohmeda Inc.) attached to a face-mask. The TCD system (PMD150 Spencer Technologies, Inc.) was used to monitor BFV in ACA and MCA. The ACA and MCA was insonated from the temporal windows by placing the 2-MHz probe in the temporal area above the zygomatic arch. Each probe was positioned to record the maximal BFV and fixed at the desired angle using a 3-dimensional positioning system to stabilize the probes. Systolic, diastolic, and mean BFV was detected from the envelope of the arterial flow waveforms. Continuous physiological monitoring of ECG, BP, BFV, and CO_2, monitoring was done during all procedures. All analog signals were recorded at 500 Hz using Labview NIDAQ (National Instruments Data Acquisition System 64 Channel/100 Ks/s, Labview 6i, Austin, TX) on a Pentium Xeon 2 GHz dual processor computer that was in use at the SAFE Laboratory, and stored for offline processing. Beat-to-beat heart rate was determined from the R-wave on the ECG, and systolic and diastolic BP was determined from the corresponding maximum and minimum of the BP waveform. Systolic, diastolic, and mean BFV were detected from the envelope of the BFV waveforms. All data was visually inspected for accuracy of R-wave detection, artifacts, and occasional extrasystoles that were removed using a linear interpolation algorithm. Respiration and CO_2 signals were equidistantly resampled at 50 Hz.

Cerebral vasoreactivity to CO_2 and pressure challenges

Hyperventilation and CO_2 rebreathing. The subject rested supine for 10 minutes with continuous monitoring of ECG, beat-to-beat BP, BFV in ACA and MCA, respiration, and CO_2. The subject then hyperventilated to reduce CO_2 to 25 mm Hg for 3 minutes. The subject breathed a mixture of 5% CO_2 and 95% air from a rebreathing bag to increase CO_2 above baseline to 45 mm Hg for 3 minutes, followed by a 5-minute rest to equilibrate CO_2.

Cerebral autoregulation to blood pressure challenges

Head-up tilt. The subjects rested supine for 10 minutes and then the table was tilted to 80° for 10 minutes. The tilt test was interrupted if symptoms of pre-syncope or blurred vision occur, at which point the affected subject was returned to the supine position.

Sit-to-stand test. Subjects sat on the chair for 5 minutes with continuous monitoring with their legs elevated at 90 degrees in front of them on a stool to reduce venous pooling. Subjects stood for 3 minutes with eyes open with continuous signal acquisition on force platform, and the trial was repeated with the cognitive challenge (number subtraction test).

Data processing and image analysis for transcranial Doppler studies - Aim 1b

Primary end points were mean BFV, CO_2 reactivity, and the BP-BFV phase shift between spontaneous oscillations during baseline and head-up tilt. The secondary end point was BP and BFV change during the sit-to-stand test in the DM and control groups**. CO_2 reactivity** was measured as the slope of regression between BFV and CO_2 changes during baseline, hyperventilation, and CO_2 rebreathing.

Multimodal pressure flow analysis: BP-BFV phase shift

To quantify the dependency between CBF and systemic pressure, we developed a novel computational method called multimodal pressure flow (MMPF) analysis.[55] The MMPF is based on an improved ensemble empirical mode decomposition algorithm that allowed us to better decompose the BP and BFV signals to intrinsic modes that correspond to oscillations at specific time scales.[54] Therefore, we were able to study BP and BFV fluctuations over a longer period of time during supine rest and head-up tilt without the active participation of a subject. We measured the BP-BFV phase shift (i) during the Valsalva maneuver using previously acquired datasets and (ii) during spontaneous BP oscillations during supine rest in diabetes subjects (see Preliminary Results section C3, Figures 5 and 6).

Head-up tilt. Regression analysis was used for evaluation of **static autoregulation** over 10 minutes of head-up tilt. Regression analysis of BP-BFV change between the supine and upright positions [46] is a robust method for evaluation of cerebral autoregulation.[75,76] Beat-to-beat BP and BFV time series were visually inspected, artifacts were removed, and data was averaged over 30-second intervals. We plotted BFV change against BP change during the tilt and fit a linear regression line. The regression coefficient was also obtained for the coefficient of determination ($R^2 \geq 0.75$). Our studies with autoregulation during head-up tilt have shown that the coefficients of determination (R^2) can identify autoregulation failure (positive correlation) and that the slope of regression provides an index of severity of such failure. The percentage change in BP and BFV relative to baseline was also calculated.

Sit-to-stand test. To quantify changes in mean BP and mean BFV during the sit-to-stand test, we computed the difference between the mean baseline value (averaged over 5 minutes) and the standing value at the time of the diastolic BP nadir (average of 5 values surrounding the nadir) for each trial, and then averaged the values for the two trials. The change in BFV relative to the change in BP was determined by dividing individual changes in flow velocity by the associated change in pressure.

Ophthalmologic examination

Ophthalmologic examination was done at the Beetham Eye Institute at the Joslin Diabetes Center using the Joslin Vision Network (JVN). The JVN video-digital retinal imaging system was used to score diabetic retinopathy and to identify other significant abnormalities in the retina.[2, 3] The JVN has been validated against the accepted standard for retinal imaging (seven-standard field 35-mm slide stereoscopic photography). Diabetic retinopathy was diagnosed from the true color, stereoscopic, high-resolution images obtained by nonmydriatic retinal fundus camera with operating characteristics modified to optimize performance for low light level imaging of the retina without pupil dilatation. These digital-video retinal images were transmitted to a central telemedicine reading center for interpretation and retinopathy severity assessment (0 = normal to 4 = severe retinopathy with additional findings).[4,5, 7]

Statistical analysis

Beat-to-beat cardiovascular and BFV data for all test conditions, BP-BFV phase shifts for baseline and head-up tilt, and CO_2 reactivity values were summarized using descriptive statistics, and one-way ANOVA was be used for comparisons between the groups. The least square models and multivariate mixed models was employed to analyze the data with mean BFV as the dependent variable, group (DM vs. control) as the independent variable, and test condition, and age and sex as co-variants. The effects of A1C, DM duration, adiposity, and co-morbidities was explored separately. CO_2 vasoreactivity and BP-BFV phase shift during baseline and tilt were evaluated using the same approach. To evaluate the effect of BP during tilt and sit-to-stand test on BFV, we used a regression model with cerebral BFV as the dependent variable and mean BP as the independent variable. These models are more flexible and account for repeated measures, missing data, and any interaction between covariates.

Power for Aim 1b. The minimum difference in mean BFV between the control and DM groups that is of clinical interest to detect during baseline is 10.4 cm/s. Using a two-sample t-test with significance level of 0.05, it was estimated that a total sample size of 120 subjects would allow us to achieve 96% power to detect a difference in BFV measured during baseline, tilt, or CO_2 rebreathing between the DM and control groups. Sample size calculations are based on BFV standard deviations of 15.0 and 14.1 cm/s for the DM and control groups, respectively, obtained from our pilot data. We aimed to have 83% power to detect a 0.43 cm/s/mm Hg difference in the CO_2 vasoreactivity slope of regression, based on our vasoreactivity values for the DM 1.18±0.7 vs. control 1.61±0.8 cm/s/mm Hg groups, alpha = 0.05. We had 99% power to detect a 21.9 degree difference in BP-BFV phase shift, based on our preliminary data values for the DM 14.9±8.9 vs. control 36.8±12.2 degrees; we had 99.9% power to detect a difference of 9.0 degrees between the groups.

Methods for Aim 2

Aim 2: To determine the association between inflammation markers and neuroanatomical changes in white matter.

Primary end points were inflammation markers (white blood cell count [WBC], sICAM-1, sVCAM-1, TNFα, CRP, and anti-inflammatory cytokine IL-10) and white matter atrophy and hyperintensities (WMHs). The secondary end point was white matter fractional anisotropy map in the control and the DM groups. Table 2 lists the statistical variables for the Aim 2 .

Inflammatory markers. Differential WBC, intracellular and vascular adhesion molecules (sICAM-1, sVCAM-1, TNF-α, and IL-6, IL10), and were measured from venous blood samples using the quantitative sandwich enzyme immunoassay technique (R&D Systems, Minneapolis, MN). CRP will be measured using the high sensitivity CRP assay Immulite-1000 (Diagnostic Product Corporation, Los Angeles, CA).
White matter and WMHs volumes were measured using the segmentation method from FLAIR images, as described above, in the control and DM groups. Fractional anisotropy map was calculated from DTI images.
Statistical analysis. Descriptive statistics was used to summarize the data and general linear models (MANCOVA) and non-parametric tests (when applicable) were used for comparisons between groups. General linear models were used to determine relationships between inflammation markers and the global and regional WM volume and WMHs volumes in the DM and control groups. Co-variables included in the model were age, A1C, and DM duration, adiposity (SKF and waist-to-hip ratio), co-morbidities, and their interactions or waist-hip ratio. The effects of A1C, DM duration, hypertension, co-morbidities and their interactions was also explored separately.

Power for Aim 2. Based on our preliminary data we had 99% power to detect a difference of 1.5 K/mL in WBC with a standard deviation of 1.5 using t-test two-sided, significance level 0.05. With 120 subjects, we had 80% power to detect a correlation coefficient of 0.23 or higher as significantly different from zero between subcortical WMHs volume and inflammation markers. This level of correlation was below that typically argued for substantial and clinically meaningful associations (0.30).[77]Therefore we had adequate power to detect meaningful correlations between inflammation markers and neuroanatomic changes.

Methods for Specific Aim 3

Aim 3: To determine the relationship between cortical and subcortical atrophy in fronto-temporal regions and memory and executive function measures and balance scores (the center of pressure displacement upon standing using force platform) in the DM and control groups over a 2-year follow-up.
In Aim 3 we planned to determine prospectively the association between diabetes control and decline in cerebral blood flow, cortical and subcortical brain volumes, and cognition and balance scores over a 2-year period.
The rationale for this Aim is that 1) mesiotemporal lobe atrophy has been shown to be associated with a decline in memory scores and executive dysfunction has been associated with a more widespread atrophy and 2) WMHs in the frontal lobe have been associated with balance impairment and falls.

Experimental protocol

The schedule for the initial and follow-up visits and the experimental protocol for MR imaging are described under the Methods for Aim 1 and in Table 1 and the variables are listed in Table 2. All participants should have

completed MRI and a battery of measures assessing executive function, attention, learning and memory, mood, and daily functioning, as well as a sit-to-stand test to measure balance.

Regional gray and white matter and CSF volumes were measured using the segmentation method, described in Aim 1a.

Measures of executive function: Verbal fluency, Trail Making Test, and Clock Drawing

Verbal fluency is assessed with phonemic and semantic fluency tasks. The phonemic fluency task[78] required the participant to generate as many words as possible beginning with a given letter (e.g., "S") for 1 minute. The semantic fluency task required the participant to generate items of a given semantic category (e.g., animals) for 1 minute. Appropriate reliability and validity have been shown in both older people and individuals with frontal lesions [79,80,81,82,83] and norms are available.[84,85] Dependent variables for the fluency measures include number of items generated for each of three phonemic trials (e.g., F, A, S) and the number of items generated for the semantic task (e.g., animals).

The Trail Making Test (parts A and B) is a measure of shifting attention. Participants were required to sequentially connect a series of numbered circles (A), and then to alternate between numbers and letters sequentially (e.g., A-1-B-2-C-3…). Trail Making B has been shown to be sensitive to changes in executive function and frontal lobe pathology.[86,87] Any participant who did not completed part B within the standard 5 minutes (300 seconds) allotted for the task was considered unable to complete the task.

Clock-in-a-Box (CIB)[88] is a modification of the commonly used Clock Drawing Test. The CIB was designed to be a very brief and easily administered cognitive screening measure. It was also designed to be domain specific, and initial studies investigating the validity of the CIB in the identification of early cognitive problems in individuals at risk for vascular dementia indicate that it is a sensitive measure of both memory and executive function. Performance on the CIB is based on the Executive Subscore and Memory Subscore, with a total of 4 possible points for each subscore.

Measures of attention

Digit Span (Forward and Backward subtests) is a brief task that assesses immediate memory/attention. It is administered using the standard format as described in the WAIS-III.[89] It consists of a series of digits of increasing length, some of which are to be recited as presented (Forward subtest) and some of which are to be recited in reverse order (Backward subtest). Dependent variables of interest for both the Forward and Backward tasks are based on the number of correctly recited digits.

Measures of learning and memory

The Hopkins Verbal Learning Test–Revised (HVLT-R) offers a *brief* assessment of verbal learning and memory (recognition and recall) that is easy to administer and score and is well-tolerated even by significantly impaired individuals. Its use has been validated with brain-disordered populations (e.g., Alzheimer's disease, Huntington's disease, amnesic disorders).[90] The HVLT-R consists of 12 nouns (targets) representing items from 1 of 3 semantic categories. The HVLT-R tasks include 3 learning trials, a delayed recall trial (20- to 25-minute delay), and a forced-choice delayed recognition trial. Dependent variables for the HVLT-R will include Total Recall (total number of list items learned across trials), Delayed Recall (total number of list items recalled after the delay), Retention (percentage of items from Total Recall that are subsequently recalled on Delayed Recall), and Recognition Discrimination Index (number of list items correctly identified among non-list items).

The Rey-Osterreith Complex Figure (ROCF) is a test of visual-spatial ability and visual memory that requires the participant to copy the figure and then immediately draw the figure from memory and to repeat the drawing approximately 30 minutes later. The dependent variables of interest are the amount of information immediately recalled (controlled for their copy score) and percentage retention. Figures such as the ROCF have been recommended to assess visual memory because they reduce the possibility that verbal mediation is used to assist recall.[91] Normative data have been provided.[92]

The Mini-Mental State Examination (MMSE) is a short assessment instrument used to grade cognitive mental status (orientation to time and place, registration, memory, attention and concentration, praxis, constructional and language capacity, ability to follow commands). It provides a quick and reliable quantitative assessment of cognitive state.[93] It is used widely in primary care[94,95,96] and research.[97] The inter-rater reliability of the MMSE in

the original presentation was reported as 0.83.[93] The dependent variable for the MMSE will be the total score, with a possible total of 30 points.

Measures of activities of mood and daily living

The effects of executive dysfunction on daily living will be assessed using the Behavioral Assessment of the Dysexecutive Syndrome (BADS).[98] The BADS is a 20-item questionnaire that samples areas important to daily living likely to be affected by executive dysfunction. The BADS has been shown to discriminate healthy adults from those with executive dysfunction. The Instrumental Activities of Daily Living (IADL) Scale is a traditional measure of various activities of daily living. Each IADL question is associated with 3 multiple-choice responses, with a different value associated with each answer. Responses reflecting more severe impairment are assigned a lower value (e.g., 1). The dependent variable for the IADLs will be the total score, with a possible total of 27 points. Geriatric Depression Scale (GDS) is a self-report measure of mood. The GDS contains 30 questions associated with overall mood, activity, sadness, and worry. Responses reflecting depressed mood are assigned a value of 1 with a possible total of 30 points. The dependent variable for the GDS will be the total score.

Experimental protocol for balance measures

Sit-to-stand test was performed as described in the Methods section for Aim 1b, according to the following protocol: 5 minutes sitting, 3 minutes standing with eyes open, 5 minutes sitting, and 3 minutes standing with cognitive challenge. Force displacement from the moment the feet touch the ground in x, y, and z directions was measured by the Kistler Force plate (Kistler Instrument Corp., Amherst, NY) simultaneously with ECG, BP, and TCD signals.

Center of pressure measurements. We analyzed the foot center-of-pressure (COP) signals— $x(t)$ for the mediolateral direction, $y(t)$ for the anteroposterior direction, and $r(t)=\sqrt{x^2(t)+y^2(t)}$ for the planar direction collected from subjects standing on a Kistler force plate (Type 5233A2, Kistler Instrument Corp., Amherst, NY). We calculatef traditional posturographic parameters including swept area, mean radius, maximum radius, standard deviations in the anteroposterior, mediolateral, and planar directions. To characterize dynamics of postural sway fluctuations in $x(t)$, $y(t)$ and $r(t)$ we used the stabilogram-diffusion analysis that has been derived from the random walk theory.[99,100] This approach derives COP parameters that can be directly related to the steady-state behavior and functional interaction of the neuromuscular mechanisms underlying the maintenance of upright stance.[99,100,101] At short time scales (Δt < ~1 seconds), the mean square displacements of a COP signal show a power-law form of the time intervals resembling a correlated random walk in which past increments in displacement are correlated with future increments.[102] The parameter H_{js}, called the scaling exponent, quantifies the correlation properties: if H_{js} = 0.5, there is no correlation and the increments in displacement are statistically independent; if H_{js} >0.5, there are positive correlations, wherein large increments are more likely to be followed by large increments (and vice versa for small increments); if H_{js} <0.5, there are negative correlations, wherein large increments are more likely to be followed by small increments.[103,104] The positive correlations in the COP signals suggest that the postural control system utilizes an open-loop control mechanism at small time scales. Negative correlations in the long-term region (time scales greater than ~2 seconds), indicate a close-loop controlled feedback. Two regions are separated by a crossover, in which the scaling exponents change gradually from the value in the short-term region to the value in the long-term region. Although, the crossover generally covers a narrow range of time scales, it is usually treated as a point at a time scale (Δt_x, Δt_y, Δt_r) for the reason of mathematic simplification. The position of the crossover is defined by the intersection of the lines fitted to the root mean square displacements in the two regions.

Statistical analysis

Primary end points for Aim 3a are the relation between cortical and subcortical volumes and cognitive and balance measures in control and DM groups. Cognitive function measures were the executive function subscore on CIB and Trail Making, part B, and the cognitive domain composite scores (e.g., memory, visuospatial, and frontal-executive function) that were developed for each subject using data reduction techniques based on factor analysis. **Posturographic measures are** swept area, mean radius, maximum

radius, standard deviations, and stabilogram-diffusion parameters including scaling exponents H and crossover time scales in the anteroposterior, mediolateral, and planar directions (Table 2).

Data reduction. We used methods of factor analysis to create composites for the main study variables. That is, within domain (executive function, memory, visuospatial, frontal-executive function, daily function, and metabolic disturbance) we performed a factor analysis to derive composite scores for each domain. In addition, we used structural equation modeling to characterize contribution of factors to diabetic metabolic disturbance (A1C, fasting glucose, DM duration, adiposity, microvascular and macrovascular disease, lipid profile, endothelial function, inflammation, smoking, sex, alcohol use, hypertension) (Figure 8). Because the sample size was small for factor analysis techniques, we used a method adopted from Rasch analysis.[74] The approach assumes that all factor loadings for factor indicators are equal. Variance in factor scores is provided by differences in the mean distribution of the individual indicators. For example, the executive function factor was indicated by performance on subtasks of the verbal fluency, Trail Making part B, and CIB tasks. We estimated factor models and derived factor scores using Mplus software (Muthén & Muthén, Los Angeles CA). We evaluated fit and residuals to determine if relaxing the assumptions of equality of factor loadings or the inclusion of specific indicators was necessary to derive a reliable and unidimensional composite score. This approach is analogous to, but slightly more precise than, the typical practice of converting all sub-task scores to z-scores and averaging z-scores. Missing data in individual task scores can be easily accommodated under missing at random assumptions. We will not estimate factor scores for persons with more than half of the sub-tasks missing. The result was determined to be at least one summary factor score or composite for each outcome domain. Factor models estimated at baseline were used to estimate composite scores at each repeated observation, thereby preserving the baseline metric over time and permitting meaningful analysis of change.

Statistical analysis. Descriptive statistics were used to summarize the data. One-way ANOVA and Wilcoxon tests were used for comparisons between the groups. The least square models and multivariate mixed models were used to determine relationships between brain volumes and composite executive and cognitive function scores, adjusted for age and sex. The same approach was used to analyze posturographic measures. The effects of A1C, DM duration, adiposity, hypertension, and co-morbidities were analyzed separately.

Power estimates. Based on cognitive measures from our preliminary data from 47 controls and 48 patients with diabetes, with 120 subjects, we aimed to have 99% power to detect a difference of 0.45 in executive function CIB score based on mean $\pm$ SD for control 3.72 ± 0.5 and 3.27 ± 0.8 for DM group, using a two-sample t-test and significance level 0.05. For Trail Making B, we had 99% power to detect a difference 31.7, for the control 75.7 ± 36.6 and 107.4 ± 52.1 for the DM group using a two-sample t-test and alpha level 0.05. To determine relation between brain atrophy and cognitive function, we based our power estimates on data from Manschot et al.[1] who described negative regression between subcortical atrophy (measured as distance between caudate nuclei and frontal horns) between midline-caudate nucleus distance and executive function r=-0.15 (-0.29-0.05, p<0.01) and between cortical atrophy (interhemispheric distance) and information processing speed r=-0.27 (-44 to-0.1, p<0.01) in type 2 DM. Volumetric measures that we proposed determined cortical and subcortical atrophy more accurately. With 120 subjects, we had 80% power to detect a correlation coefficient of 0.23 or higher as significantly different from zero between subcortical volume and executive function scores.

Aim 3b: To determine longitudinally if higher hemoglobin A1C levels are associated with progression of CBF dysregulation, brain atrophy, and decline in functional outcome measures.

We planned to determine prospectively whether higher hemoglobin A1C levels were associated with progression of brain atrophy, CBF dysregulation, and decline in cognitive and balance scores. We compared our measurements of regional perfusion and brain tissue volumes, using CASL and T1- and T2-weighted MRI at 3 Tesla (as described in Aim 1), and cognitive and balance measures at baseline and after 2 years in the diabetes and control groups. Data preprocessing is described in Aim 1 and Aim 2.

Statistical analysis. The primary end points are the differences in regional CBF, brain tissue volumes, and cognitive and balance scores at baseline and at the 2-year follow-up visit in the diabetes and control groups. The secondary end point is the relation between A1C and change in CBF, brain tissue volume, and functional measures in the diabetes group. First, we used MANCOVA to compare measurements values between baseline and follow-up and between the groups, including age, sex, and A1C as co-variants. Then in the diabetes group, we used linear and logistic regression models to determine relationship between A1C and change in CBF and

cognitive scores. The random effects and effects of possible confounding factors such as age, sex, adiposity, and DM duration and co-morbidities (hypertension, microvascular and macrovascular disease) and their interactions were included in this modeling approach. The same approach was used to determine relation of A1C to brain atrophy and balance measures. We expected that there will be missing data on MRI and TCD measures due to withdrawals, and subjects may drop-out for unknown reasons. We oversampled diabetes and control groups by 16.6% to account for drop-outs after a 2-year follow-up, and implemented modeling methods to model for a missing-value process and to provide valid inferences from data.[105] In the interpretation of these results, we considered the strength correlation (R^2), slope of regression using step-wise regression, p value, and significance of their interactions.

Power estimates. Power estimates were based on longitudinal volumetric MRI and cognitive decline measures in older people ,reported by Mungas et al,[106] who found that an annual average decrease in GM volume was $0.6 \pm 1.8\%$ in cognitively normal, $2.1 \pm 3.6\%$ in people with mild cognitive impairment and $2.8 \pm 5.3\%$ in cognitively impaired older adults. Our preliminary data (C2) showed that DM subjects have greater brain atrophy than age-matched controls; therefore we expected accelerated GM loss in the DM group over a 2-year follow-up. With 120 subjects, we had 87% power to detect a GM volume reduction of 1.2% over 2 years in cognitively normal subjects and 99% power to detect 4.2% change in subjects with mild cognitive decline and 5.6% change in cognitively impaired subjects, based on t-test two-sided and alpha = 0.05. We found in a diabetic group a significant positive relationship between A1C and frontal lobe atrophy (normalized CSF volume, r=0.45, p<0.0016). There was >1% increase in CSF volume in frontal lobe for each 0.5% increase in A1C, e.g., a A1C change from 6.0% to 8.5% was associated with 5% increase in frontal lobe atrophy. Our preliminary data indicated that with 60 DM patients we would have 83% power to detect differences of 10.8 mmL/100 mmg/min in global CBF measured by CASL between patients with uncontrolled vs. controlled DM (A1C > 7% 41.8 ± 12.8 mmL/100 mmg/min) and controlled diabetes (A1C < 7% 52.6 ± 14.2 mmL/100 mmg/min) based on t-test two-sided and alpha = 0.05.

Structural equation modeling technique - exploratory analysis

To explore the relationship between diabetes and the cardiovascular, behavioral, and biochemical factors related to executive dysfunction, we adopted the technique of structural equation modeling, which is suitable for complex physiologic networks with multiple inputs. The rationale for these analyses is that metabolic disturbance, arising from the combined effects of diabetes and its control and cardiovascular and behavioral risk factors, may lead to a vicious cycle of hypoperfusion, brain atrophy, and executive dysfunction. We consider these analyses exploratory, because the number of variables included in the model is large relative to the sample size. However, we anticipated that the strict eligibility criteria would lead to a relatively homogeneous sample and thereby decrease random variance and lead to stable model parameter estimates.

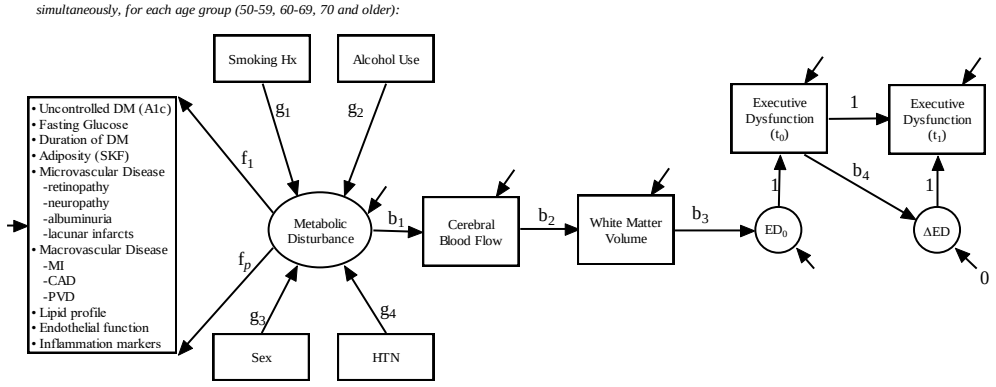

Figure 8: Structural regression model that characterizes the relationship of a latent construct termed "metabolic disturbance" to executive dysfunction at baseline (ED_0) and change in executive dysfunction (ΔED) as mediated by cerebral blood flow and brain atrophy (white matter). See text for details.

As we have shown in our preliminary results for Aim 1, our regression models revealed that baseline BFV was negatively associated with periventricular WMHs, A1C, and inflammation markers and was positively associated with systolic pressure ($R^2 = 0.86$, p<0.0001). CBF reduction in the frontal region was associated with GM atrophy across groups (p<0.0001). In the diabetic group, A1C was associated with more atrophy (CSF: p = 0.002). This modeling technique was used to explore possible mechanisms by which diabetes may lead to executive dysfunction in elderly people. Our collaborator Dr. Jones will develop a statistical model that characterizes the relationship among multiple dependent variables using structural equation modeling techniques.[107] Figure 8 shows a path diagram that incorporates three distinct model parts. The first is a

measurement model (confirmatory factor analysis) that describes a latent construct, which we have named *metabolic disturbance*, as indicated by a number of markers of DM. The second is a mediational model, wherein the effects of metabolic disturbance on executive dysfunction are viewed as mediated by cerebral blood flow and white matter volume indicators (or change in blood flow and white matter volume indicators). Finally, the model includes a latent difference score component wherein executive dysfunction at baseline (ED_0) and change in executive dysfunction (ΔED) are modeled. The metabolic disturbance latent trait is indicated by diabetes and its severity (measured with A1C and DM severity index), adiposity, and lipid profile indicators (total cholesterol, HDL, LDL) and specific measure(s) of endothelial function, inflammation, and retinopathy. The salience of each indicator for the latent metabolic disturbance variable will be determined empirically with confirmatory factor analysis: factor loadings are represented Figure 8 with f1-f*p* (where *p* is the number of indicators of metabolic disturbance retained in the final measurement model). Exogenous background variables, including sociodemographic and behavioral factors, will also be included in the model. Behavioral factors include smoking history and alcohol use. These factors contribute to metabolic disturbance severity (increasing or decreasing). These effects are represented with the structural regression parameters g1 and g2. Additionally, sex is viewed as a factor that affects levels of metabolic disturbance (g3). Note that age is not depicted as a background variable. Age will be incorporated into the model by using the multiple group approach, wherein the parameters of the model are estimated simultaneously in each of three age strata (50-59 years, 60-69 years, and $\geq$70 years). We will initially assume that all model parameters are equal across age groups, and will test differences in the model parameters across age groups by iteratively relaxing these equality constraints. We hypothesize that different aspects of the "metabolic disturbance," especially adiposity, will have different degrees of salience in different age groups. Finally, hypertension will be included as a covariate (g4).

We hypothesize a causal chain links the metabolic disturbance to executive dysfunction via decreases in cerebral blood flow (b1) and brain atrophy and white matter changes (b2). The total effect of metabolic disturbance on executive dysfunction at baseline, in the absence of a direct influence, is given by (b1*b2*b3). Change in executive dysfunction (b4) is modeled using McArdle and Hamagami's [108] latent difference score approach. Model building will proceed by first specifying and arriving at a well-fitting measurement model, then a mediation model that includes baseline executive dysfunction only, and ultimately the full model depicted in Figure 8 that adds the latent difference score model for change in executive dysfunction. After a well-fitting model is obtained, we will also explore alternative hypotheses. An important alternative model to be evaluated is that metabolic disturbance directly affects executive function, regardless of cerebral blood flow and WMHs.

This study will provide invaluable data about the effects of diabetes on cerebral perfusion that can translate into new diagnostic markers and therapeutic targets for management of diabetic brain damage and incorporated into broad initiatives for prevention of cognitive decline in older adults.
Development of instruments, methods, software and analysis programs, and databases needed for data processing will be completed during year 1 to begin cross-sectional analysis as the data are being acquired. Longitudinal analysis and modeling will be done in year 5. Study groups will be over-sampled during visit 1 to allow for drop-outs and missing data.

Reference List

1. Manschot,S.M. *et al.* Brain magnetic resonance imaging correlates of impaired cognition in patients with type 2 diabetes. *Diabetes* **55**, 1106-1113 (2006).

2. Aiello,L.M., Cavallerano,J.D., Cavallerano,A.A., & Bursell,S.E. The Joslin Vision Network (JVN) Innovative Telemedicine Care for Diabetes. *Ophthalmol. Clin. North. Am.* **13**, 213-224 (2000).

3. Bursell,S.E. *et al.* Stereo nonmydriatic digital-video color retinal imaging compared with Early Treatment Diabetic Retinopathy Study seven standard field 35-mm stereo color photos for determining level of diabetic retinopathy. *Ophthalmology* **108**, 572-585 (2001).

4. Cavallerano,A.A. *et al.* Use of Joslin Vision Network digital-video nonmydriatic retinal imaging to assess diabetic retinopathy in a clinical program. *Retina* **23**, 215-223 (2003).

5. Cavallerano,A.A. *et al.* A telemedicine program for diabetic retinopathy in a Veterans Affairs Medical Center--the Joslin Vision Network Eye Health Care Model. *Am. J. Ophtalmol* **139**, 597-604 (2005).

6. Fong,D.S., Warram,J.H., Aiello,L.M., Rand,L.I., & Krolewski,A.S. Cardiovascular autonomic neuropathy and proliferative diabetic retinopathy. *Am. J. Ophtalmol* **120**, 317-321 (1995).

7. Wilson,C., Horton,M., Cavallerano,J.D., & Aiello,L.M. Addition of primary care-based retinal imaging technology to an existing eye care professional referral program increased the rate of surveillance and treatment of diabetic retinopathy. *Diabetes Care* **28**, 318-322 (2005).

8. Bastyr,E.J.3., Price,K.L., Bril,V., & the MMBQ Study group Development and validity testing of the neuropathy total symptom score-6: questionnaire for the study of sensory symptoms of diabetic peripheral neuropathy. *Clin. Ther.* **27**, 1278-1294 (2005).

9. Bril,V. & Perkins,B.A. Validation of the Toronto Clinical Scoring System for diabetic polyneuropathy. *Diabetes Care* **25**, 2048-2052 (2002).

10. Kamimura,M.A. *et al.* Comparison of skinfold thicknesses and bioelectrical impedance analysis with dual-energy X-ray absorptiometry for the assessment of body fat in patients on long-term haemodialysis therapy. *Nephrol. Dial. Transplant.* **18**, 101-105 (2003).

11. Cohen,J. *Statistical power analysis for the behavioral sciences.*(Lawrence Erlbaum Associates, New Jersey, 1988).

12. Launer,L.J. Diabetes and brain aging: epidemiologic evidence. *Curr. Diab. Rep.* **5**, 59-63 (2006).

13. Horani,M.H. & Mooradian,A.D. Effect of diabetes on the blood brain barrier. *Curr. Pharm. Des.* **9**, 833-840 (2003).

14. Korf,E.S., White,L.R., Scheltens,P., & Launer,L.J. Brain aging in very old men with type 2 diabetes: the Honolulu-Asia Aging Study. *Diabetes Care* **29**, 2268-2274 (2006).

15. Schmidt,R. *et al.* Magnetic resonance imaging of the brain in diabetes: the Cardiovascular Determinants of Dementia (CASCADE) Study. *Diabetes* **53**, 687-692 (2004).

16. Xu,W.L., Qiu,C.X., Wahlin,A., Winblad,B., & Fratiglioni,L. Diabetes mellitus and risk of dementia in the Kungsholmen project: a 6-year follow-up study. *Neurology* **63**, 1181-1186 (2004).

17. Task Force on Community Preventive Services Strategies for reducing morbidity and mortality from diabetes through health-care system interventions and diabetes self-management education in

community settings. A report on recommendations of the task force on community preventive services. *National Center for Chronic Disease Prevention and Health Promotion, MMWRI* **50**, (2001).

18. Makimattila,S. *et al.* Brain metabolic alterations in patients with type 1 diabetes-hyperglycemia-induced injury. *J Cereb Blood Flow Metab* **24**, 1393-1399 (2004).

19. Brownlee,M. The pathobiology of diabetic complications. *Diabetes* **54**, 1615-1625 (2006).

20. Keymeulen,B. *et al.* Regional cerebral hypoperfusion in long-term type 1 (insulin-dependent) diabetic patients: relation to hypoglycaemic event. *Nucl. Med. Commun.* **16**, 10-6 (1995).

21. Kannel,W.B., Kannel,C., Paffenbarger,R.S.J., & Cupples,L.A. Heart rate and cardiovascular mortality: The Framingham study. *Am. Heart J.* **113**, 1494 (1987).

22. Gunning-Dixon,F.M. & Raz,N. The cognitive correlates of white matter abnormalities in normal aging: a quantitative review. *Neuropsychology* **14**, 224-232 (2000).

23. Vazquez,L.A. *et al.* Decreased plasma endothelin-1 levels in asymptomatic type I diabetic patients with regional cerebral hypoperfusion assessed by Spect. *J. Diabetes Complications* **13**, 325-331 (1999).

24. Jimenez-Bonilla,J.F. *et al.* Assessment of cerebral blood flow in diabetic patients with no clinical history of neurological disease. *Nucl Med Commun* **17**, 790-794 (1996).

25. Kadoi,Y., Saito,S., Goto,F., & Fujita,N. The effect of diabetes on the interrelationship between jugular venous oxygen saturation responsiveness to phenylephrine infusion and cerebrovascular carbon dioxide reactivity**.** *Anesth Analg* **99**, 325-331 (2004).

26. Kadoi,Y. *et al.* Diabetic patients have an impaired cerebral vasodilatory response to hypercapnia under propofol anesthesia. *Stroke* **34**, 2399-2403 (2003).

27. Wakisaka,M. *et al.* Reduced regional cerebral blood flow in aged noninsulin-dependent diabetic patients with no history of cerebrovascular disease: evaluation by N-isopropyl-123I-p-iodoamphetamine with single-photon emission computed tomography. *J. Diabetes Complications* **4**, 170-174 (1990).

28. MacLeod,K.M. *et al.* The effects of acute hypoglycemia on relative cerebral blood flow distribution in patients with type I (insulin-dependent) diabetes and impaired hypoglycemia awareness. *Metabolism* **45**, 974-980 (1996).

29. Cranston,I. *et al.* Regional differences in cerebral blood flow and glucose utilization in diabetic man: the effect of insulin. *J Cereb Blood Flow Metab* **18**, 130-140 (1998).

30. Vermeer,S.E. *et al.* Silent brain infarcts and white matter lesions increase stroke risk in the general population: The Rotterdam scan study. *Stroke* **34**, 1126-1129 (2003).

31. Schmidt,R. *et al.* White matter lesion progression: a surrogate endpoint for trials in cerebral small-vessel disease. *Neurology* **63**, 139-144 (2004).

32. Musen,G. *et al.* Effects of type 1 diabetes on gray matter density as measured by voxel-based morphometry. *Diabetes* **55**, 326-333 (2006).

33. Ikram,M.K. *et al.* Retinal vessel diameters and cerebral small vessel disease: the Rotterdam Scan Study. *Brain*182-188 (2006).

34. Vermeer,S.E., Prins,N.D., den Heijer,T., Koudstaal,P.J., & Breteler,M.M. Silent brain infarcts and the risk of dementia and cognitive decline. *N. Engl. J. Med.* **27**, 1215-1222 (2003).

35. deGroot,J.C. *et al.* Cerebral white matter lesions and subjective cognitive dysfunction: the Rotterdam Scan Study. *Neurology* **56**, 1539-1541 (2001).

36. Meyer,J.S., Rogers,R.L., Judd,B.W., Mortel,K.F., & Sims,P. Cognition and cerebral blood flow fluctuate together in multi-infarct dementia. *Stroke* **19**, 163-169 (2003).

37. DeCarli,C. & et al. The effect of white matter hyperintensity volume on brain structure, cognitive performance, and cerebral metabolism of glucose in 51 healthy adults. *Neurology* **45**, 2077-2084 (1995).

38. Looi,J.C. & Sachdev,P.S. Differentiation of vascular dementia from AD on neuropsychological tests. *Neurology* **53**, 670-678 (1999).

39. Laughton,C.A. *et al.* Aging, muscle activity, and balance control: physiologic changes associated with balance impairment. *Gait Posture* **18**, 101-108 (2003).

40. Norris,J.A., Marsh,P.M., Smith,I.J., Kohut,R.I., & Miller,M.E. Ability of static and statistical mechanics posturographic measures to distinguish between age and fall risk. *Journal of Biomechanics* **38**, 1263-1272 (2005).

41. Nardone,A., Grasso,M., & Schieppati,M. Balance control in peripheral neuropathy: are patients equally unstable under static and dynamic conditions? *Gait Posture* **23**, 364-373 (2006).

42. Tell,G.S., Lefkowitz,D.S., Diehr,P., & Elster,A.D. Relationship between balance and abnormalities in cerebral magnetic resonance imaging in older adults. *Arch. Neurol.* **55**, 73-9 (1998).

43. Whitman,G.T. & Tang,T. A prospective study of cerebral white matter abnormalities in older people with gait dysfunction. *Neurology* **57**, 990-994 (2001).

44. Baloh,R.W., Ying,S.H., & Jacobson,K.M. A longitudinal study of gait and balance dysfunction in normal older people. *Arch. Neurol.* **60**, 835-839 (2003).

45. Mehagnoul-Schipper,D.J., Colier,W.N., & Jansen,R.W. Reproducibility of orthostatic changes in cerebral oxygenation in healthy subjects aged 70 years and older. *Clin. Physiol.* **21**, 77-84 (2001).

46. Novak,V., Novak,P., Spies,J.M., & Low,P.A. Autoregulation of cerebral blood flow in orthostatic hypotension. *Stroke* **29**, 104-111 (1998).

47. Novak,V. *et al.* Cerebral blood flow velocity and periventricular white matter hyperintensities in type 2 diabetes. *Diabetes Care* **29**, 1529-1534 (2006).

48. Last,D. *et al.* Global and regional effects of type 2 diabetes mellitus on brain tissue volumes and cerebral vasoreactivity . *Diabetes Care* **30**, 1193-1199 (2007).

49. Knopman,D.S., Mosley,T.H., Catellier,D.J., & Sharrett,A.R. Cardiovascular risk factors and cerebral atrophy in a middle-aged cohort. *Neurology* **65**, 876-881 (2005).

50. Schmidt,M.I. *et al.* Markers of inflammation and prediction of diabetes mellitus in adults (Atherosclerosis Risk in Communities study): a cohort study. *Lancet* **15**, 1649-1652 (1999).

51. Boyd,C.M. *et al.* Clinical practice guidelines and quality of care for older patients with multiple comorbid diseases: implications for pay for performance. *JAMA* **294**, 716-724 (2005).

52. Cukierman,T., Gerstein,H.C., & Williamson,J.D. Cognitive decline and dementia in diabetes--systematic overview of prospective observational studies. *Diabetologia. 2005* **48**, 2460-2469 (2005).

53. Wei,X. *et al.* Quantitative analysis of MRI signal abnormalities of brain white matter with high reproducibility and accuracy. *J. Magn. Reson. Imaging* **15**, 203-209 (2002).

54. Huang,N.E. *et al.* The empirical mode decomposition method and the Hilbert spectrum for non-stationary time series analysis. *Proc. Roy. Soc. London* **A454**, 903-995 (1998).

55. Novak,V. *et al.* Multimodal pressure-flow method to assess dynamics of cerebral autoregulation in stroke and hypertension. *BioMedical Engineering OnLine* **3**, 39 (2004).

56. Collignon,A. *et al.* Automated multimodality image registration based on information theory in *Information Processing in Medical Imaging* (eds. Bizais,Y., Barillot,C. & DiPaola,R.) 263-274 (Kluwer Academic Publishers, Dordrecht, 1995).

57. Wells,W.M., III, Viola,P., Atsumi,H., Nakajima,S., & Kikinis,R. Multi-modal volume registration by maximization of mutual information. *Med. Image Anal.* **1**, 35-51 (1996).

58. Van Leemput,K., Maes,F., Vandermeulen,D., & Suetens,P. Automated model-based tissue classification of MR images of the brain. *IEEE Trans. Med. Imaging* **18**, 897-908 (1999).

59. D'Agostino,E., Maes,F., Vandermeulen,D., & Suetens,P. *Non-rigid atlas-to-image registration by minimization of class-conditional image entropy*2004).

60. Wahlund,L.O. *et al.* A new rating scale for age-related white matter changes applicable to MRI and CT. *Stroke* **32**, 1318-1322 (2001).

61. Williams,D.S., Detre,J.A., Leigh,J.S., & Koretsky,A.P. Magnetic Resonance Imaging of Perfusion Using Spin Inversion of Arterial Water. *Proceedings of the National Academy of Sciences USA* **89**, 212-216 (1992).

62. Williams,K. & MacLean,C. Transcranial assessment of maternal cerebral blood flow velocity in normal vs. hypertensive states. Variations with maternal posture. *Journal of Reproductive Medicine* **39**, 685-688 (1994).

63. Alsop,D.C. & Detre,J.A. Reduced transit-time sensitivity in non-invasive magnetic resonance imaging of human cerebral blood flow. *Journal Cerebral Blood Flow Metabolism* **16**, 1236-1249 (1996).

64. Ye,F.Q. *et al.* H2150 PET validation of steady-state arterial spin tagging cerebral blood flow measurements in humans. *Magn Reson Med* **44**, 450-456 (2000).

65. Alsop,D.C. & Detre,J.A. Multisection cerebral blood flow MR imaging with continuous arterial spin labeling. *Radiology* **208**, 410-416 (1998).

66. Detre,J.A. *et al.* Noninvasive magnetic resonance imaging evaluation of cerebral blood flow with acetazolamide challenge in patients with cerebrovascular stenosis. *J. Magn. Reson. Imaging* **10**, 870-875 (1999).

67. Detre,J.A. *et al.* Noninvasive MRI evaluation of cerebral blood flow in cerebrovascular disease. *Neurology* **50**, 633-641 (1998).

68. Salat,D.H. *et al.* Age-related alterations in white matter microstructure measured by diffusion tensor imaging. *Neurobiology of Aging* **26**, 1215-1227 (2005).

69. Salat,D.H. *et al.* White matter alterations in cerebral amyloid angiopathy measured by diffusion tensor imaging. *Stroke* **37**, 1759-1764 (2006).

70. Pierpaoli,C. & Basser,P.J. Toward a quantitative assessment of diffusion anisotropy. *Magn Reson Med* **36**, 893-906 (1996).

71. Cheng,P. *et al.* Evaluation of the GTRACT diffusion tensor tractography algorithm: A validation and reliability study. *NeuroImage* **31**, 1085 (2006).

72. Kwan,J., Lunt,M., & Jenkinson,D. Assessing dynamic cerebral autoregulation after stroke using a novel technique of combining transcranial Doppler ultrasonography and rhythmic handgrip. *Blood Press Monit.* **9**, 3-8 (2004).

73. in *A First Course in factor Analysis.* (eds. Comrey,A. & Lee,H.) (Lawrence Erlbaum Assoc, Inc, 1992).

74. in *Probabilistic models for some intelligence and attainment tests.* (ed. Rasch,G.) (Danish Institute of Educational Research, Copenhagen, 1960).

75. Werner,C. *et al.* Cerebral blood flow and cerebral blood flow velocity during angiotensin-induced arterial hypertension in dogs. *Canadian Journal of Anaesthesia* **40**, 755-760 (1993).

76. Bondar,R.L. *et al.* Simultaneous cerebrovascular and cardiovascular responses during presyncope. *Stroke* **26**, 1794-1800 (1995).

77. in *Statistical power analysis for the behavioral sciences.* (ed. Cohen,J.) (Academic Press, New York, 1969).

78. Benton,A.L. & Hamsher,K. *Multilingual Aphasia Examination*(University of Iowa, Iowa City, 1976).

79. de Rosiers,G. & Kavanagh,D. Cognitive assessment in closed head injury: Stability, validity and parallel forms for two neuropsychological measures of recovery. *International Journal of Clinical Neuropsychology* **9**, 162-173 (1987).

80. Miceli,G., Caltagirone,C., Gainotti,G., Massullo,C., & Silveri,M.C. Neuropsychological correlates of localized cerebral lesions in non-aphasic brain-damaged patients. *Journal of Clinical Neuropsychology* **3**, 53-63 (1981).

81. Perret,E. The left frontal lobe of man and the supression of habitual responses in verbal categorical behavior. *Neuropsychologia* **12**, 323-330 (1974).

82. Ramier,A.-M. & Hacaen,H. Role respectif des attaintes frontales et la lateralisation lesoinelle dans les deficits de la "fluence verbale.". *Revue Neurologique* **123**, 17-22 (1970).

83. Snow,W.G., Tierney,M.C., Zorzitto,M.L., Fisher,R.H., & Reid,D.W. One year test-retest of reliability of selected tests in older adults. 1988. New Orleans, Annual Meeting of the International Neuropsychological Society.
Ref Type: Conference Proceeding

84. Read,E.E. *Neuropsychological assessment of memory in early dementia: Normative data for a new battery of memory tests*(University of Victoria, Brittish Columbia, 1987).

85. Yeudall,L.T., Fromm,D., Reddon,J.R., & Stefanyk,W.O. Normative data stratified by age and sex for 12 neuropsychological tests. *Journal of Clinical Psychology* **42**, 918-946 (1986).

86. Pugh,G.K. & Lipsitz,L.A. Selective impairment of frontal-executive cognitive function in African-Americans with cardiovascular risk factors. *JAGS*(2003).

87. Libon,D. *et al.* Age, executive functions, and visuospatial functioning in healthy older adults. *Neuropsychology* **8**, 38-43 (1994).

88. Grande,L.J., Milberg,W., Rudolph,J., Gaziano,M., & McGlinchey,R. A timely screening for executive functions and memory. *Journal of the International Neuropsychological Society* **11**, 31 (2005).

89. Wechsler D. Wechsler Memory Scale-Revised (manual). 1987. New York, Psychological Corporation.
Ref Type: Audiovisual Material

90. Shapiro,A., Benedict,R., Schretlen,D., & Brandt,J. Construct and concurrent validity of the Hopkins Verbal Learning Test--Revised. *Clinical Neuropsychologist* **13**, 348-358 (1999).

91. Lezak,M.D., Howieson,D.B., Loring,D.W., Hannay,H.J., & Fischer,J.S. *Neuropsychological Assessment Fourth Edition*(Oxford University Press, London, 2004).

92. Spreen,O. & Strauss,E. *A compendium of neuropsychological tests: Administration, norms, and commentary*(Oxford University Press, London, 1991).

93. Folstein,M.F., Folstein,S.E., & McHugh,P.R. Mini-mental state. A practical method for grading the cognitive state of patients for the clinician. *J Psychiatr Res* **12**, 189-198 (1975).

94. Goldschmidt,T.J., Mallin,R., & Still,C.N. Recognition of cognitive impairment in primary care outpatients. *South Med J* **76**, 1264-1270 (1983).

95. Murden,R.A., McRae,T.D., Kaner,S., & Bucknam,M.E. Mini-Mental State exam scores vary with education in blacks and whites. *J Am Geriatr Soc* **39**, 149-155 (1991).

96. Tangalos,E.G. *et al.* The Mini-Mental State Examination in general medical practice: clinical utility and acceptance. *Mayo Clin Proc* **71**, 829-837 (1996).

97. George,L., Landerman,R., Blazer,D., & Anthony,J.in *Cognitive Impairment, in Psychiatric Disorders in America* (eds. Robins,L. & Regier,D.) 291-327 (The Free Press, New York, 1991).

98. Burgess,P., Alderman,N., Wilson,B., Evans,J., & Emslie,H. The Dysexecutive Questionnaire in *Behavioral Assessment of the Dysexecutive System* (eds. Wilson,B., Alderman,N., Burgess,P., Emslie,H. & Evans,J.) (Thames Valley Test Company, Bury St. Edmunds, U.K., 1996).

99. Collins,J.J. & De Luca,C.J. Open-loop and closed-loop control of posture: a random-walk analysis of center-of-pressure trajectories. *Exp. Brain Res.* **95**, 308-318 (1993).

100. Collins,J.J. & De Luca C.J Random walking during quiet standing. *Phys. Rev. Lett.* **73**, 764-767 (1994).

101. Collins,J.J. & De Luca,C.J. Upright, correlated random walks: A statistical-biomechanics approach to the human postural control system. *Chaos* **5**, 57-63 (1995).

102. Mandelbrot,B.B. & Van Ness,J.W. Fractional Brownian motions, fractional noises and applications. *SIAM Review* **10**, 422-437 (1968).

103. Feder,J. *Fractals*(Plenum Press, New York, 1988).

104. Saupe,D. Algorithms for random fractals in *The Science of Fractal Images* (eds. Peitgen,H.-O. & Saupe,D.) 71-136 (Springer-Verlag, New York, 1988).

105. Little,R. Modeling the drop-out mechanism in repeated measures studies. *Journal of the American Statistical Association* **431**, 1112-1121 (1995).

106. Mungas,D. *et al.* Longitudinal volumetric MRI change and rate of cognitive decline. *Neurology* **23**, 565-571 (2005).

107. Bollen,K.A. *Structural equations with latent variables*(John Wiley & Sons Inc. New York, 1989).

108. Mc Ardle,J. & Hamagami,F. Latent difference score structural equation models for linear dynamic analyses with incomplete longitudinal data. in *New methods for the analysis of change* (eds. Collins,L. & Sayer,A.) 137-176 (American Psychological Associaiton, Washington, D.C., 2002).